SECURITY CLASSIFICATION OF THIS PAGE

REPORT DOCUMENTATION PAGE

Form Approved OMB No. 0704-0188

1a. REPORT SECURITY CLASSIFICATION: UNCLASSIFIED	1b. RESTRICTIVE MARKINGS: NONE
2a. / 2b. / 4. I: AD-A217 398	3. DISTRIBUTION/AVAILABILITY OF REPORT: APPROVED FOR PUBLIC RELEASE; DISTRIBUTION UNLIMITED.
	5. MONITORING ORGANIZATION REPORT NUMBER(S): AFIT/CI/CIA-89-031
6a. NAME OF PERFORMING ORGANIZATION: AFIT STUDENT AT UTAH ST UNIV / 6b. OFFICE SYMBOL (If applicable):	7a. NAME OF MONITORING ORGANIZATION: AFIT/CIA
6c. ADDRESS (City, State, and ZIP Code):	7b. ADDRESS (City, State, and ZIP Code): Wright-Patterson AFB OH 45433-6583
8a. NAME OF FUNDING/SPONSORING ORGANIZATION / 8b. OFFICE SYMBOL (If applicable):	9. PROCUREMENT INSTRUMENT IDENTIFICATION NUMBER
8c. ADDRESS (City, State, and ZIP Code):	10. SOURCE OF FUNDING NUMBERS: PROGRAM ELEMENT NO. / PROJECT NO. / TASK NO. / WORK UNIT ACCESSION NO.

11. TITLE (Include Security Classification) (UNCLASSIFIED)
SOLAR CYCLICAL TREND STUDY OF THE MID-LATITUDE, QUIET-TIME, MERIDIONAL, NEUTRAL WINDS AT WINTER SOLSTICE CONDITIONS

12. PERSONAL AUTHOR(S)
RONALD LEE BRENINGER

13a. TYPE OF REPORT	13b. TIME COVERED	14. DATE OF REPORT (Year, Month, Day)	15. PAGE COUNT
THESIS/DISSERTATION	FROM _____ TO _____	1989	81

16. SUPPLEMENTARY NOTATION
APPROVED FOR PUBLIC RELEASE IAW AFR 190-1
ERNEST A. HAYGOOD, 1st Lt, USAF
Executive Officer, Civilian Institution Programs

17. COSATI CODES			18. SUBJECT TERMS (Continue on reverse if necessary and identify by block number)
FIELD	GROUP	SUB-GROUP	

19. ABSTRACT (Continue on reverse if necessary and identify by block number)

90 02 01 019

20. DISTRIBUTION/AVAILABILITY OF ABSTRACT	21. ABSTRACT SECURITY CLASSIFICATION
☒ UNCLASSIFIED/UNLIMITED ☐ SAME AS RPT. ☐ DTIC USERS	UNCLASSIFIED

22a. NAME OF RESPONSIBLE INDIVIDUAL	22b. TELEPHONE (Include Area Code)	22c. OFFICE SYMBOL
ERNEST A. HAYGOOD, 1st Lt, USAF	(513) 255-2259	AFIT/CI

DD Form 1473, JUN 86 — Previous editions are obsolete. — SECURITY CLASSIFICATION OF THIS PAGE

AFIT/CI "OVERPRINT"

SOLAR CYCLICAL TREND STUDY OF THE MID-LATITUDE, QUIET-TIME, MERIDIONAL, NEUTRAL WINDS AT WINTER SOLSTICE CONDITIONS

by

Ronald Lee Breninger, Capt, USAF

A thesis submitted in partial fulfillment
of the requirements for the degree

of

MASTER OF SCIENCE

UTAH STATE UNIVERSITY
Logan, Utah

1989

(81 Pages)

SOLAR CYCLICAL TREND STUDY OF THE MID-LATITUDE, QUIET-TIME, MERIDIONAL, NEUTRAL WINDS AT WINTER SOLSTICE CONDITIONS

by

Ronald Lee Breninger, Capt, USAF

A thesis submitted in partial fulfillment
of the requirements for the degree

of

MASTER OF SCIENCE

UTAH STATE UNIVERSITY
Logan, Utah

1989

(81 Pages)

SOLAR CYCLICAL TREND STUDY OF THE MID-LATITUDE, QUIET-TIME, MERIDIONAL, NEUTRAL WINDS AT WINTER SOLSTICE CONDITIONS

by

Ronald Lee Breninger, Capt, USAF

A thesis submitted in partial fulfillment
of the requirements for the degree

of

MASTER OF SCIENCE

in

Soil Science and Biometeorology

(Aeronomy)

Approved:

Kent S. Miller
Major Professor

Lawrence E. Hipps
Committee Member

Gene W. Kelaus
Committee Member

Lawrence H. Rietveld
Dean of Graduate Studies

UTAH STATE UNIVERSITY
Logan, Utah

1989

ACKNOWLEDGEMENTS

This study was made under the direction of Dr. Kent L. Miller of the Center of Atmospheric and Space Sciences (CASS). I extend my sincere appreciation to Dr. Miller for his encouragement and help. Additionally, I wish to thank Dr. Gene Adams of CASS and Dr. Larry Hipps of the Department of Soil Science and Biometeorology for their participation in the preparation of this thesis. Their suggestions and critical review of this work have enhanced the qualitiy of this investigation. A special word of thanks goes to Teri Olsen for her time and care expended in the compilation of this thesis.

Finally, to my wife, Glenda, for her patience and support in fulfilling this assignment, I extend a husband's gratitude.

Ronald Lee Breninger

TABLE OF CONTENTS

LIST OF TABLES

LIST OF FIGURES

ABSTRACT

Solar Cyclical Trend Study of the Mid-latitude, Quiet-Time, Meridional, Neutral Winds at Winter Solstice Conditions

by

Ronald Lee Breninger, Master of Science

Utah State University, 1989

Major Professor: Dr. Kent L. Miller
Department: Center for Atmospheric and Space Sciences

Located within the region of the thermosphere is the major portion of the ionosphere. Distribution of the ionospheric plasma within this region is a function of atmospheric mass and energy transport. At mid-latitudes, absorption of UV and EUV radiation are two of the principle ionization and heating sources within the thermosphere. The level of UV and EUV radiation is directly related to the amount and intensity of solar activity. As with temperature variations, other thermospheric properties, such as particle density, and circulation phenomena, such as zonal and meridional winds, indicate a dependence on the level of solar activity. Systematic measurements of thermospheric winds are made on a limited basis by a sparse network of Fabry-Perot interferometers, incoherent scatter radars, and satellites. For the current study, the component of the

neutral wind along the magnetic meridian is derived from ground-based ionosonde measurements of the F2 peak layer height. Meridional wind variations with respect to location, universal time, and level of solar activity are the focal points on this investigation. The primary timescale of interest covers a period of one solar cycle, from 1977 to 1987. Data from one station have been extended to 1965 to study the repetitive nature of solar activity on the meridional winds.

The F2 layer height is determined by using scaled ionosonde critical frequencies and an empirical equation developed by Bradley and Dudeney. Ionospheric parameters relating to the F2 layer height were determined from quiet to moderate solar indices using the Field Line Interhemispheric Plasma (FLIP) ionospheric model of Richards and Torr.

Results of this study indicate a definite variation of wind speed and direction, which correlates with changing levels of solar activity. It is hoped that the results of this study will aid current efforts to develop ionospheric models and enhance their forecasting capabilities.

(81 pages)

CHAPTER I

INTRODUCTION

Overview

For the purposes of this study, the thermosphere is the region above the mesopause, where the neutral gas temperature begins to increase with height. It extends up to the exosphere, where the neutral temperature is constant. Located within the thermosphere is the major portion of the ionosphere, which, under the influence of electric and magnetic fields, directly effects the energetics and dynamics of the neutral atmosphere. Distribution of the ionospheric plasma within this region is a function of atmospheric mass and energy transport [Blum and Harris, 1973].

Absorption of ultraviolet (UV) and extreme ultraviolet (EUV) solar radiation are two of the principle ionization and heating sources of the mid-latitude thermosphere. The level of UV and EUV radiation that reaches the earth's upper atmosphere is largely dependent on the amount and intensity of solar activity [Lakshimi et al., 1988] and causes large temperature variations in the thermosphere, as seen in Figure 1 [Banks and Kockarts, 1973; Jacchia and Slowey, 1973; Hedin and Mayr, 1987]. A similar solar cycle effect is expected in other thermospheric properties, such as particle density, and circulation phenomena, such as

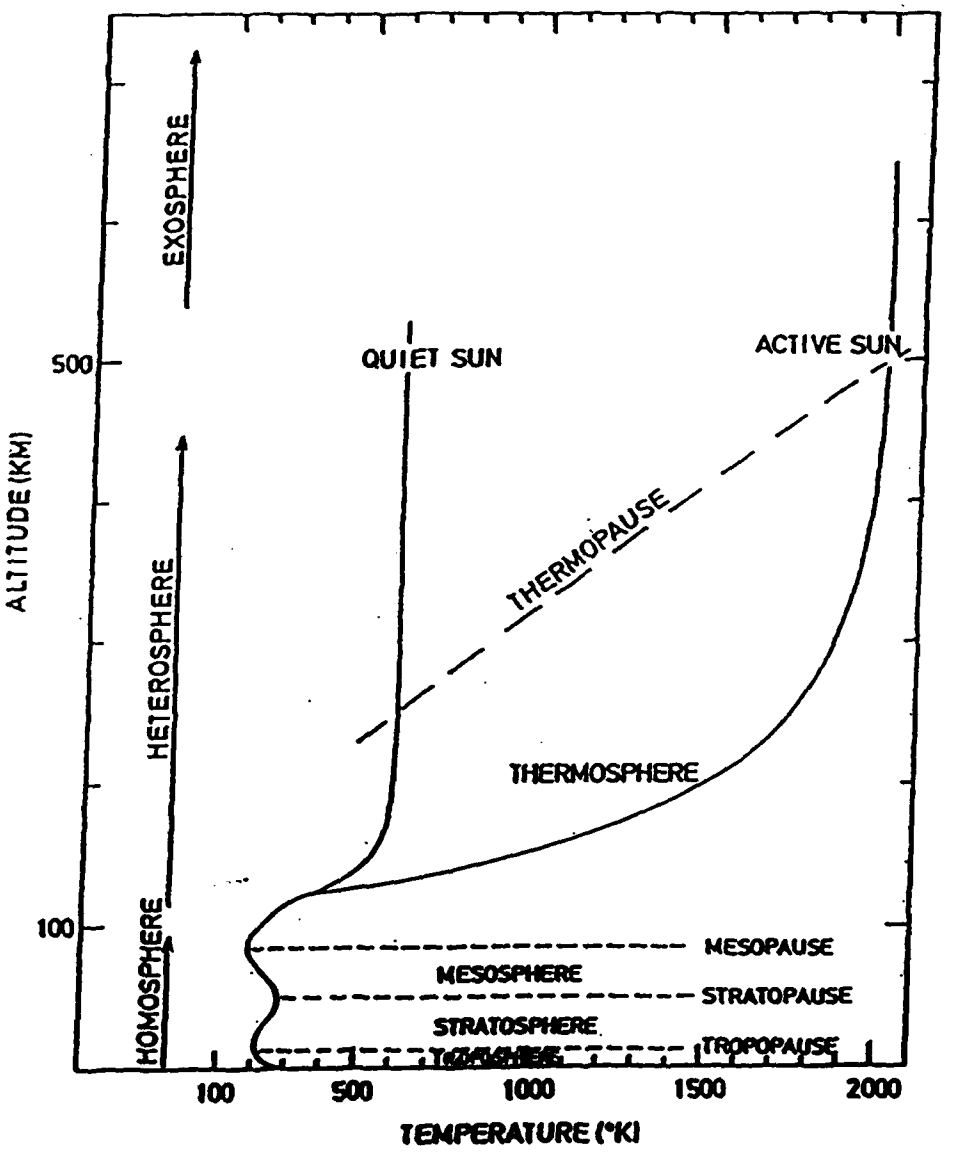

Fig. 1. Vertical temperature profile of the earth's atmosphere. [Reprinted by permission of Academic Press from Banks and Kockarts 1973].

zonal and meridional winds [Hernandez and Roble, 1976; Hernandez, 1982].

Thermal energy, which is deposited in the upper atmosphere, is transported by vertical heat conduction to the lower atmosphere, where radiative cooling processes dominate. Forcing functions due to UV and EUV radiation, coupling pro-cesses of the thermosphere-magnetosphere systems, and coupling processes of the thermosphere-lower atmosphere systems exhibit spatial and temporal variations. A combination of thermospheric winds from solar radiation inputs, electric field convection processes, and ion drag effects cause frictional interactions of Joule heating and viscous energy dissipation [Mayr and Harris, 1978; Mayr and Harris 1979; Forbes, 1982; Hedin and Mayr, 1987].

Problem Statement

Systematic measurement of thermospheric winds is made on a limited basis by a sparse network of Fabry-Perot interferometers [Hernandez and Roble, 1976], incoherent scatter radars [Salah and Holt, 1974], and by satellite measurements of the Doppler shift of the airglow spectra [Herraro et al., 1988]. A method of deriving the component of the neutral wind along the magnetic meridian, using ground-based ionosonde measurements of the F2 peak layer height as developed by Miller et al. [1986], greatly enhances the capabilities of studying mid-latitude circulation phenomena. Meridional winds determined by this

method are a function of location, universal time, and the level of solar activity. These variations are the primary areas of concern in this research effort.

Objectives of the Investigation

The primary objective of this investigation is to conduct a trend study of the mid-latitude, quiet-time, meridional neutral winds over the period of two solar cycles, which span the time period of 1965 to 1987, at winter solstice conditions. The use of archived ionosonde data, from the World Data Center at Boulder, Colorado [Conkright and Brophy, 1982], allows for such a study to be conducted on a global scale. The method of determining meridional neutral winds is based on measurement of the height of the maximum electron density of the F layer [Miller et al., 1986]. The height of the maximum electron density, hmax or hmF2 as it is referred to, increases or decreases as collisions between ions and neutral atmospheric particles force the ions to move parallel to the magnetic field in the direction of the meridional component of the neutral wind [Miller et al., 1987]. Natural downward diffusion of ionization is either enhanced or opposed, depending on the direction of the meridional neutral wind. In response to such activity, the maximum ion density occurs at a higher or lower level of the ionosphere with respect to the "balance height" of no neutral wind.

A second objective of this study is to conduct a sta-

tistical error analysis of the technique of Miller et al. [1986] for determination of the meridional neutral wind. The error in the meridional neutral wind is determined to be a function of time, change in the layer height with respect to wind speed, hmax, and the balance height, which are the variables used in the calculation of the meridional winds. The definitions of these variables are iterated in a later portion of this paper. A finite differencing technique, using the root mean square error of each of the variables, is used to establish the uncertainty in the meridional neutral wind, U [Baird, 1962].

The third objective is to develop a representation of the meridional neutral winds by the use of a grid layout of ionosonde stations. Stations selected for this study form a latitudinal chain and a longitudinal chain, as seen in Figure 2. Additional site-specific information is contained in Appendix A. Such a network of stations allows for the investigation of the meridional neutral winds in a spatial coordinate frame [Challinor and Eccles, 1971]. The result of this study provides location-specific variations of the meridional neutral winds with respect to solar cycle variations.

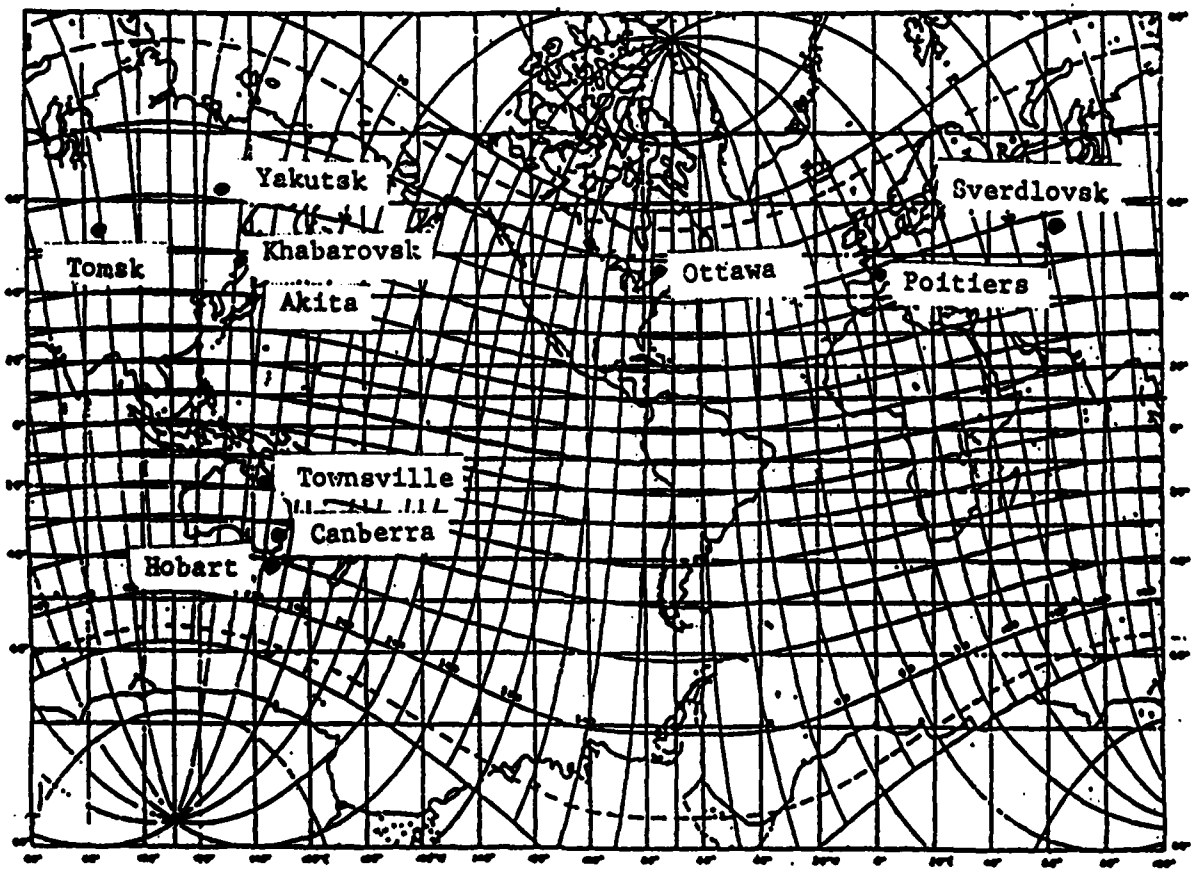

Fig. 2. Ionosonde locations on a centered dipole coordinate frame superposed on a geographic mecator projection [adopted from Chernosky et al., 1965].

CHAPTER II

REVIEW OF LITERATURE

Meridional Winds

Thermal expansion of the atmosphere by day forms a diurnal bulge [Rishbeth, 1972; Salah and Holt, 1974], which gives rise to horizontal pressure gradients, which in turn drive horizontal winds. These thermospheric winds, to some degree, are subject to the Coriolis effect due to the earth's rotation. They are even more strongly influenced by frictional forces due to the viscosity of the air and collisions between ions and neutral atmospheric particles. Additional information on this subject is provided in a later portion of this chapter. Ions exert a drag on the air motion because of the strong ties with the earth's magnetic field. Ion drag is a major limiting factor of the wind speeds at thermospheric heights [Rishbeth, 1972].

Thermospheric winds blow from the hottest part of the thermosphere to the coldest part and therefore blow across the poles and zonally around the earth in the low latitude regions. The winds move F-region ions and electrons in the direction of the earth's magnetic field, with the overall effect of the wind being dependent on its orientation with respect to the magnetic field.

Daytime (poleward) and nighttime (equatorward) meridional winds cause a lowering of the daytime F2 layer and

raising of the nighttime F2 layer of the ionosphere beyond the normal, diurnal variations caused by production, recombination, and diffusion processes [Rishbeth, 1966; Rishbeth, 1972]. The variation of the F2 peak layer height due to the influence of the meridional neutral winds is nearly linear, under steady state conditions [Miller et al., 1986; Miller and Torr, 1987]. The neutral wind, as determined by such a method, is given by the relationship

$$U = \frac{ho - hmax}{\alpha} \qquad (1)$$

where U ≡ horizontal component of the neutral wind along a magnetic meridian,

hmax ≡ measured F2 peak layer height,

ho ≡ calculated balance height of the F2 peak density at U = 0, as calculated by the Richards-Torr ionospheric model [Young et al., 1980],

α ≡ calculated value of $(h_{RT2} - h_{RT1})/(u_2 - u_1)$, as determined by a linear regression technique of the Richards-Torr ionospheric model [Young et al., 1980],

h_{RT1}, h_{RT2} ≡ layer height as determined by the Richards-Torr ionospheric model [Young et al., 1980], and

u_1, u_2 ≡ inputed meridional winds of the Richards-Torr ionospheric model [Young et al., 1980].

Derivation of equation (1) neglects electric field effects on the F2 layer height. There is no component of the electric field parallel to the magnetic field at mid-latitudes which affects the layer height [Stubbe and Chandra, 1970; Rishbeth 1972; Miller et al., 1986; Miller et al., 1987; Miller and Torr, 1987]. At mid-latitudes, it is the east-

west component of the earth's electric field which affects the F2 layer height. The apparent meridional wind, U, is therefore a combination of the meridional wind, U_y, and the zonal electric field wind [Hanson and Patterson, 1964; Hernandez and Roble, 1976; Miller et al., 1986; Miller et al., 1987], or

$$U = U_y + \frac{E_x}{B \sin I} \qquad (2)$$

For the northern hemisphere, U_y is the magnetically northward component of the actual neutral wind; E_x the eastward component of the electric field, E; B the magnitude of the magnetic field, B; and I the inclination of the magnetic field. At mid-latitudes, the effect of the second term of equation (2) is generally small in comparison to the first term [Stubbe and Chandra, 1970; Salah and Holt, 1974; Miller et al., 1987]. Additional details on this point are included in the section on ionospheric models. The area of greatest uncertainty of U occurs at sunrise due to the effects of photochemistry on the F2 layer height [Hanson and Patterson, 1964; Rishbeth, 1966]. Photoionization establishes a minimum value of hmax at this time of the day [Miller et al., 1986]. The daytime F2 layer height is most sensitive to changes in the meridional wind, since there is a balance between diffusive and photochemical processes occurring within the ionosphere. It is less sensitive at night, when the F layer is maintained by downward diffusion.

Seasonal and Solar Cycle Variations

The major contributor to thermospheric circulation, at mid-latitudes, is heating by absorption of solar UV and EUV radiation [Rishbeth, 1972; Dickinson et al., 1977; Hedin and Mayr, 1987], with some amplification resulting from high latitude heat sources. At winter solstice conditions, a summer to winter interhemispheric flow regime is established. This flow regime is reinforced by a high latitude heat source in the summer hemisphere and opposed in the winter hemisphere at F region heights above 150 km [Roble et al., 1977; Babcock and Evans, 1979]. Below 150 km a summer to winter flow pattern is established at all latitudes.

Solar UV and EUV heating is approximately two times lower at solar minimum than it is at solar maximum. Corresponding to this solar cycle effect, a factor of 4.5 difference has been noted in the strength of the high latitude heat source between solar maximum and solar minimum conditions [Roble et al., 1977]. This variation is computed based on a requirement for modeling of the temperatures and meridional winds to match observations made at solar cycle maximum and minimum conditions. The high latitude heat source variation is the result of the interaction on the solar wind and the earth's magnetic field [Dickinson et al., 1977].

In a study by Roble et al. [1977], at winter solstice, a temperature difference of 325 K, at solar maximum, and

200 K, at solar minimum, occurs between the summer and winter poles. Latitudinal variations of the mean molecular mass are also greatest at solstice conditions with a maximum value occurring in the summer hemisphere. This variation is due, in part, to the large mixing ratios of the heavier atmospheric constituents found in the winter hemisphere.

Under solstice conditions, at solar maximum, the entire thermospheric circulation below 150 km exhibits the summer to winter hemispheric flow pattern as seen in Figure 3. Above 200 km, the meridional wind strength intensifies in an equatorial direction with a maximum strength occurring at the solstice time period [Roble et al., 1977]. Under solstice conditions, the auroral zone heating in the summer hemisphere combines with solar EUV heating to drive a Hadley cell circulation, which transports air across the equator from the summer to winter hemisphere. This flow is resisted by an oppositely directed flow in the winter hemisphere due to auroral heating in that hemisphere [Babcock and Evans, 1979]. The reverse cell acts to decrease the poleward winds in the winter hemisphere, which are driven by solar heating in the summer hemisphere, and results in an assymetric pattern in the meridional winds at mid-latitudes [Roble et al., 1977; Babcock and Evans, 1979]. The strength of this circulation and the location of the boundary of circulation reversal, as illustrated in Figure 3, are expected to be dependent on the level of geomagnetic activity [Hernandez

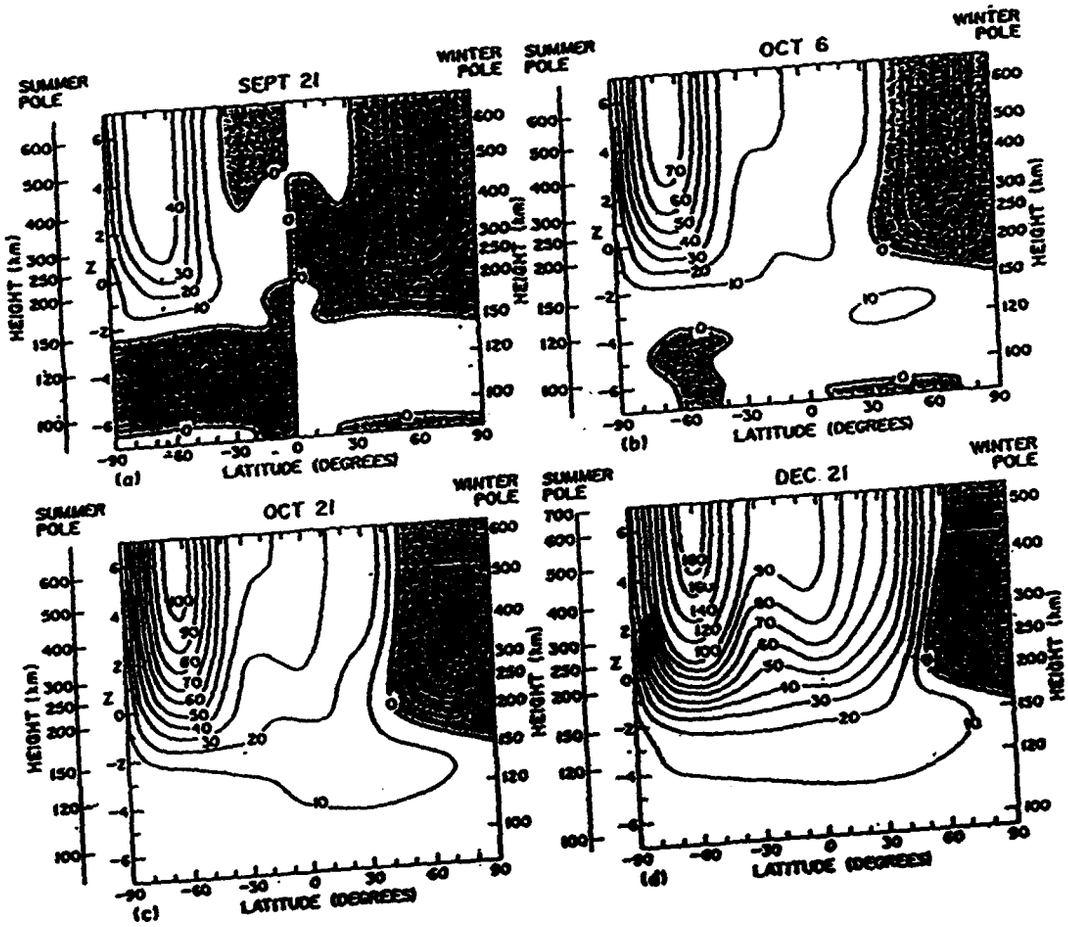

Fig. 3. Meridional wind component for various time periods of the year, at solar maximum. Units are in meters per second [from Roble et al., 1977].

and Roble, 1977; Roble et al., 1977].

Thermospheric, meridional winds at solar minimum and at winter solstice conditions flow from the summer to winter hemisphere at all altitudes and latitudes [Hernandez and Roble, 1977]. The magnitude of these winds, as seen in Figure 4, is nearly two times lower than the values found at solar maximum. This difference is attributable to the diminished high latitude heat source, which is needed to create a reverse circulation [Roble et al., 1977].

Observations of sunspot numbers provide a means of prediction of ionospheric parameters, such as the F region critical frequency, foF2, and the F region peak layer height, hmF2 [Smith and King, 1981]. Drawbacks to using the monthly mean sunspot number, R_{12}, are the saturation effects and the variation of foF2 for the same value of R_{12} in different phases of the solar cycle [Hedin and Mayr, 1987; Lakshimi et al., 1988]. Results of a study by Lakshimi et al. [1988] of the values of foF2 versus EUV flux (170-190 Å) and the sunspot number, R_{12}, show no saturation effects in the winter solstice time frame at low latitudes. Such is not the case for mid-latitude regions, as neither the use of EUV radiation flux or R_{12} provide a greater degree of accuracy in the determination of foF2. Additionally, the results of the work of Babcock and Evans [1979] and Lakshimi et al. [1988] indicate that an increase in solar activity increases the pressure gradients, which drive thermospheric

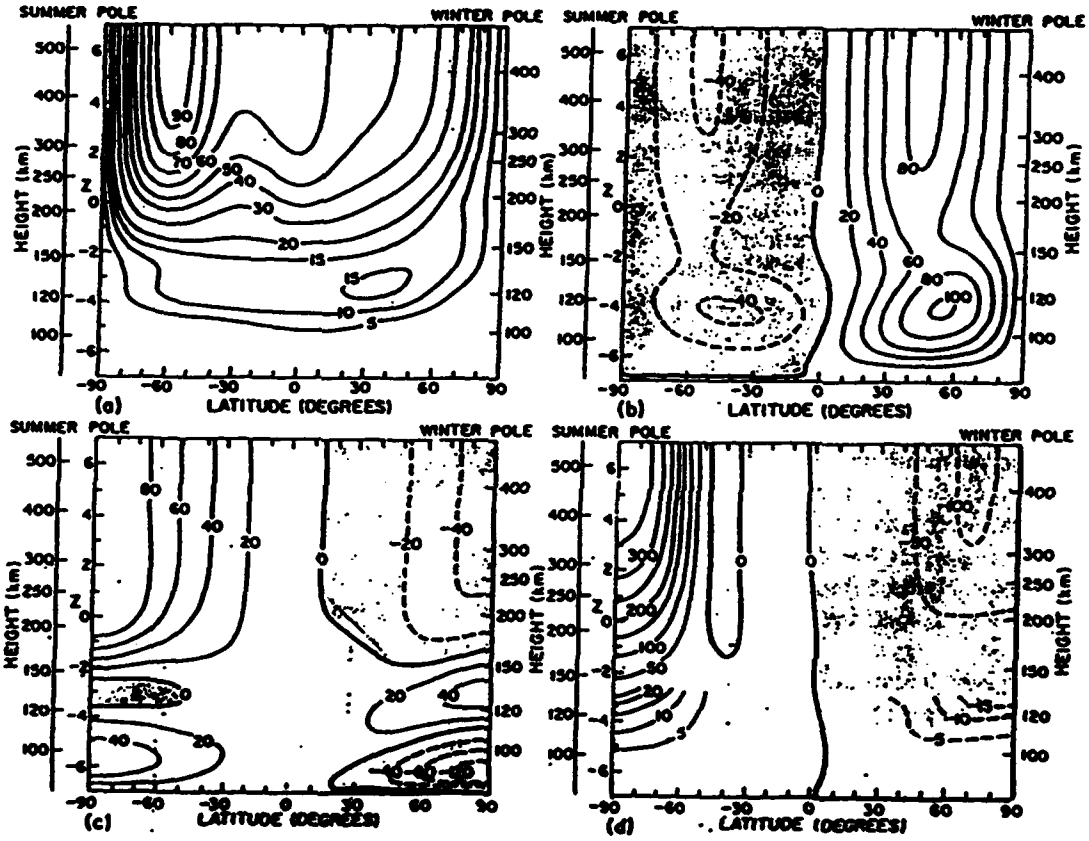

Fig. 4. Contours of temperature and winds for winter solstice at solar minimum; (a) meridional winds (m/s), (b) zonal winds (m/s), (c) temperature (K), and (d) vertical winds (cm/s) [from Roble et al., 1977].

winds, but, at the same time, an increase in the charged particle population leads to increased ion drag, which inhibits the winds [Hedin and Mayr, 1987]. In general, as the level of solar activity decreases, daytime wind speeds increase because ion drag decreases more rapidly than the pressure gradient force [Rishbeth, 1972].

Based on a total of 64 geomagnetically quiet days, from 1970 to 1975, Babcock and Evans [1979] found a decrease in the annual mean meridional wind, at Millstone Hill, of 25 m/s equatorward to 0 m/s. They conclude that the decrease in wind speed is indicative of a decrease in auroral forcing relative to the level of solar forcing at solar minimum. Babcock and Evans [1979] carried out a least squares curve fitting of the mean meridional wind, at the Millstone Hill observatory in Boston, Massachusetts, and established a correlation with the three month average 10.7 cm solar radio flux, F10.7A [Jacchia and Slowey, 1973; Hedin and Mayr, 1987]. At Millstone Hill, for solar maximum the mean summer wind is approximately 75 m/s equatorward while a winter wind of 30 m/s poleward was calculated. For solar minimum, the average winter wind increases to 40 m/s and the duration of the summer equatorward wind is reduced in comparison to that of solar maximum conditions while the speed was relatively unchanged.

Ionospheric Models

In the thermosphere, molecules collide frequently so that the air may be considered to be a fluid, which is sub-

ject to the hydrodynamic equations of motion. Furthermore, the air can be treated as a single fluid because the differential motion of the constituents is much less than the overall wind speed [Rishbeth, 1972; Blum and Harris, 1973].

The equation of motion may be represented as:

$$\frac{d\mathbf{U}}{dt} + 2\boldsymbol{\Omega} \times \mathbf{U} = \nabla P - \nu_{ni}(\mathbf{U} - \mathbf{V}) + \frac{\mu}{\rho} \nabla^2 \mathbf{U} + \mathbf{g} \qquad (3)$$

(a) (b) (c) (d) (e) (f)

where term (a) is acceleration, (b) Coriolis term, (c) pressure gradient, (d) ion drag, (e) viscous drag, and (f) gravity. For the terms of equation (3) $\mathbf{U}$ is the neutral wind velocity, $\mathbf{V}$ is the ion drift velocity, $\boldsymbol{\Omega}$ the earth's angular velocity, ν_{ni} the neutral-ion collision frequency, μ/ρ the kinematic viscosity, and $\mathbf{g}$ the acceleration due to gravity.

In order to calculate $\mathbf{U}(t)$ in a coordinate frame which is fixed with respect to the earth, the Coriolis and centripetal accelerations due to rotation of the earth must be included in the equation of motion for determination of the motion of the air, $d\mathbf{U}/dt$. Local acceleration, $\partial\mathbf{U}/\partial t$, differs from this quantity due to the transport of momentum past a given point. According to the chain rule for derivatives, $d/dt = \partial/\partial t + (\mathbf{U} \cdot \nabla)$. A non-linear advection term, $(\mathbf{U} \cdot \nabla)\mathbf{U}$, results from application of this definition to the wind velocity $\mathbf{U}$.

Centripetal acceleration is generally neglected because it is constant in magnitude and direction at any given

latitude. The non-linear advection term is small if U is much smaller than the earth's rotational speed, Ω, and therefore may generally be neglected. The non-linear advection term may be significant for large values of U and large spatial gradients, $\nabla \cdot \mathbf{U}$, as can occur near the periods of sunrise and sunset [Rishbeth, 1972; Salah and Holt, 1974].

The pressure gradient force is not exactly vertical and therefore is comprised of both horizontal and vertical components. It is the horizontal components which provide the driving force for zonal and meridional winds. The vertical component, though largest in magnitude, is counterbalanced by the gravitational force and has little effect on air motion.

Viscous forces are created if wind shears exist. It is generally the vertical wind shear which is of concern and therefore the viscous drag term of equation (3) becomes $(\mu/\rho)\partial^2\mathbf{U}/\partial z^2$, which allows for diffusion effects to be considered. In other words, the momentum of air tends to diffuse so as to smooth the velocity-height profile. This term is important at high altitudes where the density of the atmospheric particles is small and the kinematic viscosity is therefore large [Blum and Harris, 1973; Salah and Holt, 1974; Hedin and Mayr, 1987].

The collision frequency for momentum transfer, ν_{ni}, is comparable to the average frequency with which a neutral

particle experiences a collision with an ion. By Newton's Third Law, $\rho_n \nu_{ni} = \rho_i \nu_{in}$, where ρ_i and ρ_n are ion and neutral densities. At the F2 peak altitude, where 1 part in 1000 of the air is ionized, $\nu_{in} \approx 1\ s^{-1}$ and $\nu_{ni} \approx 10^{-3}\ s^{-1}$. The time constant within which an ion transfers motion to the neutral is $1/\nu_{ni} \approx 1000$ s [Rishbeth, 1972].

The four principal causes of ion motion in the F layer are plasma diffusion, neutral horizontal winds, vertical thermal expansion and contraction of the atmosphere, and drifts due to electric fields generated by dynamo action in the E layer. Their relative magnitudes, in terms of their contributions to **V**, at mid-latitudes are given in Table 1 [Rishbeth 1972; Salah and Holt, 1974]. If the ion gyrófrequency, ω_i, is much greater than the collision frequency, ν_{in}, as is the case at F layer altitudes, then plasma diffusion, the neutral horizontal winds, and thermal expansion and contraction produce ion motion which is parallel to the geomagnetic field [Roble and Dickinson, 1974]. Ion drift due to the electric field is perpendicular to the magnetic field, **B**.

An approximation of the ion motion is made by setting the ion velocity equal to the meridional component of the neutral wind, **U**, or

$$\mathbf{V} = \frac{(\mathbf{U} \cdot \mathbf{B})\mathbf{B}}{B^2} \qquad (4)$$

Ion drag then depends only on the orientation of the magnetic field and is a function of the inclination, I, and

Table 1. Magnitude of the Principle Causes of Ion Motion Relative to the Ion Drift Velocity [based on Rishbeth, 1972].

CAUSE OF ION MOTION	MAGNITUDE
Plasma Diffusion	10 m/s
Neutral Horizontal Winds	100 m/s (nighttime) 30 m/s (daytime)
Vertical Thermal Expansion and Contraction	3 m/s
Dynamo Induced Drifts	30 m/s

declination, D, angles [Rishbeth, 1972; Roble and Dickinson, 1974].

Plasma diffusion must be accounted for due to electrostatic force between ions and electrons. Ion diffusion velocities are the sum of the ion and electron partial pressures. Collisions between electrons and ions and between electrons and neutrals have little effect on the ion drift velocity and the overall air motion. This is due to the large differences in mass of the electrons as compared to that of the ions and neutral particles.

Based on the above discussion, a modified equation of motion can be given as

$$\frac{d\mathbf{U}}{dt} = \nabla P + \frac{\mu}{\rho}\frac{\partial^2 \mathbf{U}}{\partial z^2} - \nu_{ni}(\mathbf{U} - \mathbf{V}) - 2\Omega \times \mathbf{U} + \mathbf{g} \qquad (5)$$

which can be resolved into horizontal and vertical com-

ponents. The vertical component reduces to the hydrostatic equation and is generally neglected in ionospheric models [Rishbeth, 1972; Young et al., 1980]. In such cases a model atmosphere, such as MSIS [Hedin, 1983], is adopted so that density is treated as a known quantity. The Coriolis effect, relative to the ion drag effect, is not a major factor at night, when the peak density, NmF2, becomes small. In general, when $f = 2\Omega \sin \phi$, in which ϕ is the geographic latitude, is greater than ν_{ni} then the Coriolis effect is an important factor. This situation is found below 150 km and above 400 km. However, above 400 km, viscosity outweighs both the Coriolis effect and ion drag [Rishbeth, 1972].

The Richards-Torr ionospheric model makes use of modified momentum and energy equations [Hanson and Patterson, 1964; Rishbeth, 1972; Schunk, 1974; Hernandez and Roble, 1976; St. Maurice and Schunk, 1977; Schunk and Nagy, 1978]. Such modifications restrict the use of this model to the mid-latitude ionosphere, which is a region of closed magnetic field lines. Additionally, the mid-latitudes are a region where electric field convection effects are small in comparison to that of meridional winds [Stubbe and Chandra, 1970]. For this model, the plasma consists of the two major ions of O^+ and H^+, electrons, and some minor ions in a neutral atmosphere whose major constituents are O, O_2, N_2, and H. Modifications of the momentum and energy equations

are based on the following conditions [Young et al., 1980]:

1) Species temperature and flow velocity differences are small, allowing one to neglect the stress and non-linear acceleration terms and to use linear collision terms.

2) Density and temperature gradients, perpendicular to the earth's magnetic field, are neglected.

3) Ion and electron temperature distributions are isotropic.

4) Electric field convection of the flux tube is omitted and restricts useage to quiet or moderate geomagnetic conditions [Miller et al., 1987]. Such conditions are maintained in the current investigation, as seen in Appendix B.

The final result is a set of six equations consisting of a photoelectron two stream equation, ion and electron energy equations, ion and electron momentum equations, and the continuity equation [Young et al., 1980]. The Richards-Torr ionospheric model simulates interhemispheric plasma flow in an entire flux tube, which spans the mid-latitude between magnetically conjugate points, in the F region of the ionosphere, as illustrated in Figure 5 [Young et al., 1980]. Of an additional note, neutral atmospheric parameters within the model are calculated by the MSIS-83 model [Hedin, 1983]. Selection of the Richards-Torr ionospheric model is based on its incorporation of seasonal, solar cycle, and diurnal variations. An additional criterion is its ability to respond to varying intensities

1, 1*: Boundary region (Density is continuous)
2, 2*: Boundary region (Density and flux are continuous)
A, A*: Regions of local chemistry
B, B*: Regions of ion diffusion (parabolic density equations)
C : Region of diffusive equilibrium

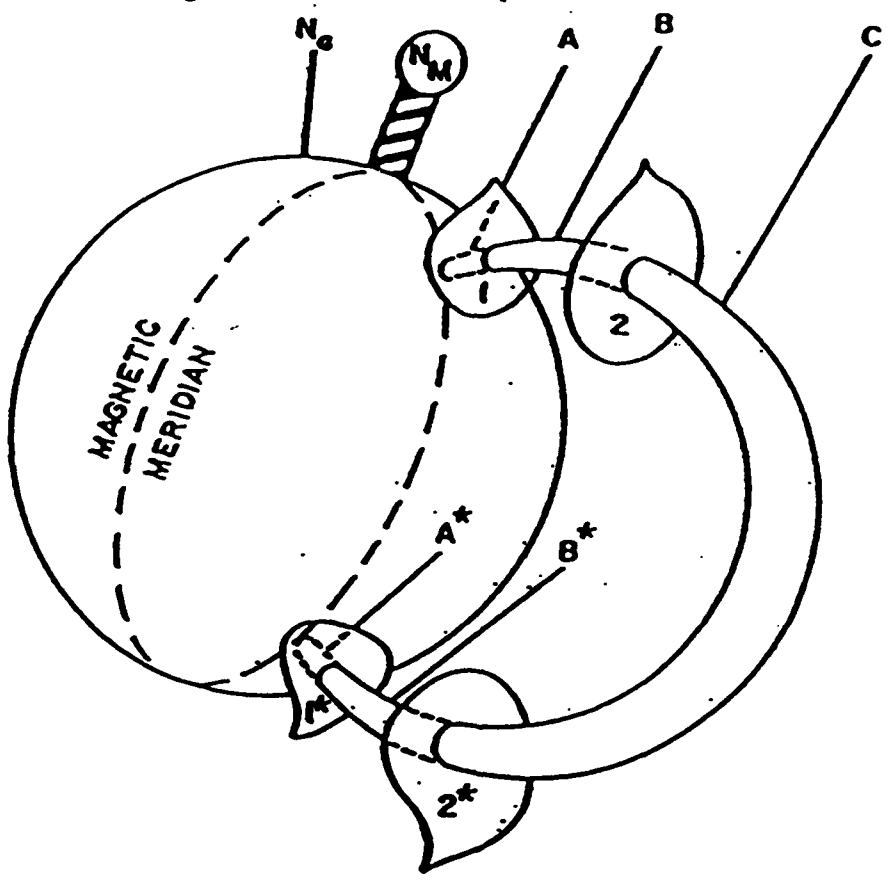

Fig. 5. Regions and boundaries of the Richards-Torr ionospheric model. [Reprinted by permission of Pergamon Press from Young et al., 1980].

of geomagnetic disturbances [Young et al., 1980].

The Bradley-Dudeney model ionosphere provides a means of determining hmax, or hmF2, from ionosonde measurements of the ionosphere. The three parameters, which are inputs into this model, are the critical frequencies, foE and foF2, and the maximum usable frequency factor for a path of 3000 km for transmission by the F2 layer of the ionosphere, M(3000)F2. Measurment of these parameters is made on a continuous 24-hour basis by over 126 stations, which store their data in the World Data Center at Boulder, Colorado.

Figure 6 provides a schematic of the Bradley-Dudeney model ionosphere [Bradley and Dudeney, 1973] which consists of parabolic E and F layers with a linear region of electron concentration between them. The calculation of hmax from this model is restricted to values of x, the ratio of foF2 to foE, greater than 1.7. In this model, hmax is defined as

$$hmax = a\,[M(3000)F2]^{b} \qquad (6)$$

where $$a = 1890 - \frac{355}{x - 1.4}$$

and $$b = (2.5x - 3)^{-2.35} - 1.6$$

Discrepancies with the true height profiles are of the order of ± 10 km [Bradley and Dudeney, 1973; Dudeney, 1983] for the quiet, daytime, mid-latitude ionosphere. Application of this model is based on the selection of such locations and geomagnetic conditions. The error in the Bradley-Dudeney formula of equation (6) is likely to be greater than

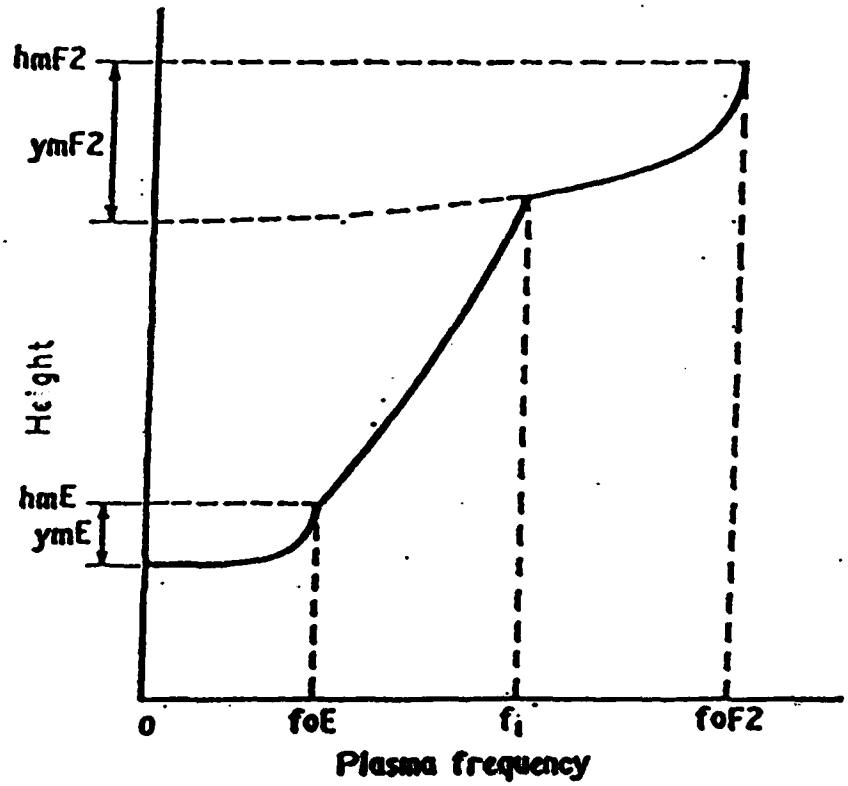

Fig. 6. Bradley-Dudeney ionosphere. The ordinate and abscissa are linear in height and frequency. [Reprinted by permission of Pergamon Press from Bradley and Dudeney, 1973].

± 10 km for nighttime conditions due to its dependency on the ratio of foF2 to foE. Nighttime measurements of foE are not available due to the decay of the E region. For this and other problems of measurement of foE, such as sporadic E, the values of foE used in this investigation are approximated from the IRI model densities as

$$foE = 9 \times 10^{-3} \sqrt{NmE} \qquad (7)$$

where NmE is the electron number density at the E peak layer height [Chen, 1984].

CHAPTER III

METHOD

Procedure

As stated in the title, the primary objective of this investigation is a trend study of the mid-latitude, quiet-time, meridional neutral winds. The period of study covers two solar cycles, during the years of 1965 to 1987, with a majority of the emphasis on the years of 1977 to 1987. Use of the additional solar cycle, 1965 to 1976, will be as verification of information gleaned from the primary period of this study. In terms of seasonal effects on the thermospheric winds, only the winter solstice time period, and in particular the month of January, will be considered.

The method of determining the values of the meridional wind is based on the works of Rishbeth [1972] and Miller et al. [1986]. Additional information on this subject is contained in Chapter II in the section on meridional winds. Figure 7 provides a schematic flow digram of the method employed in the determination of the meridional neutral winds.

As stated in equation (1), a linear relationship exists between the meridional neutral wind, U, and the F2 peak layer height, hmax or hmF2. Determination of the height, hmax, is based on the empirical relationship, developed by Bradley and Dudeney [1973], as stated in equation (6).

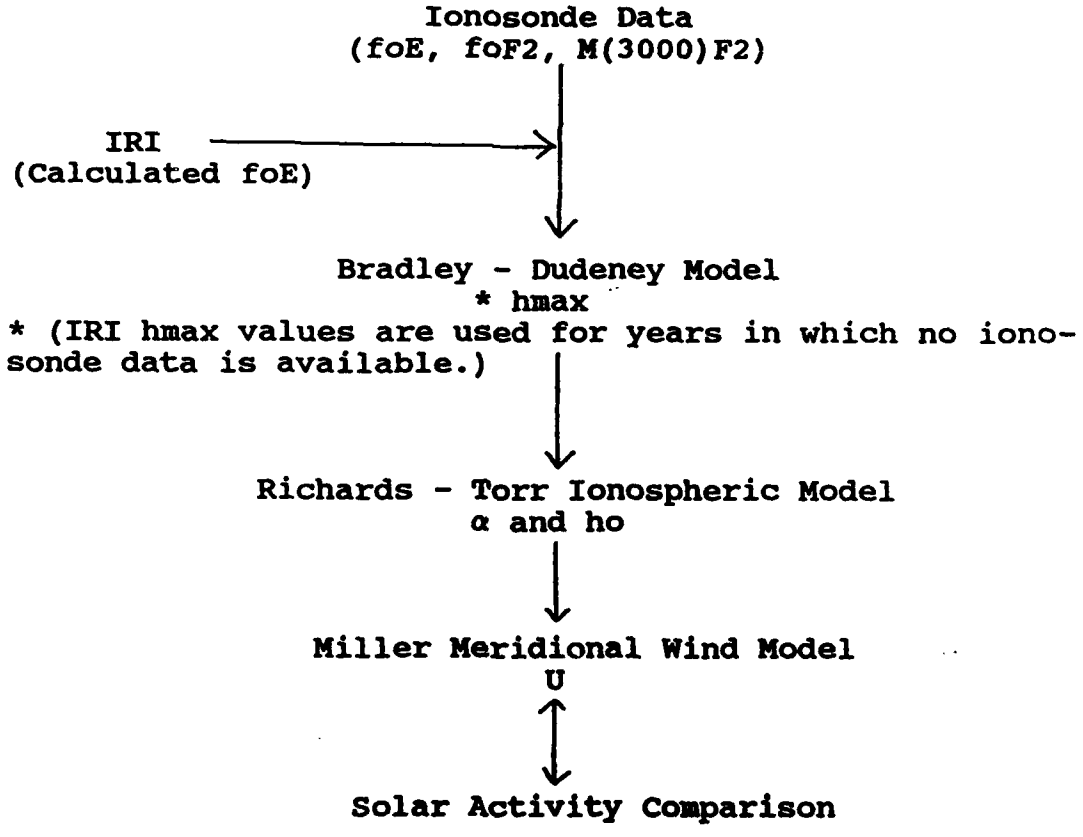

Fig. 7. Schematic of data analysis for the solar cyclical trend study of the meridional neutral winds.

Archived ionosonde data, from the World Data Center at Boulder, Colorado, of the critical frequencies, foE and foF2, and the maximum transmission frequency, M(3000)F2, provide the observed input for this investigation. However, due to problems in the measurement of foE, as previously stated, the E layer critical frequency used throughout this investigation is calculated from the IRI model E layer density, NmE. The use of such data is based on comparison of the calculated values and measured values of foE in terms of their relative impact on the ratio of foF2 to foE, which is required for determination of hmax. The variance between the IRI model values and measured values of foE is generally less than 5 to 10% and does not significantly change the final wind values. For the locations and time periods where ionosonde data are unavailable, as stated in Appendix A, the IRI model value of hmax has been used in the determination of the meridional winds [Miller et al., 1989]. Of and additional note, throughout this investigation an average of the ten most quiet days is used for the determination of hmax, ho, and α. This technique applies to the calculation of both the input ionosonde frequencies of the Bradley-Dudeney model and the geomagnetic indices used by the Richards-Torr ionospheric model. Selection of the ten most quiet days show no significant variance in terms of Kp index, as seen in Figure 8.

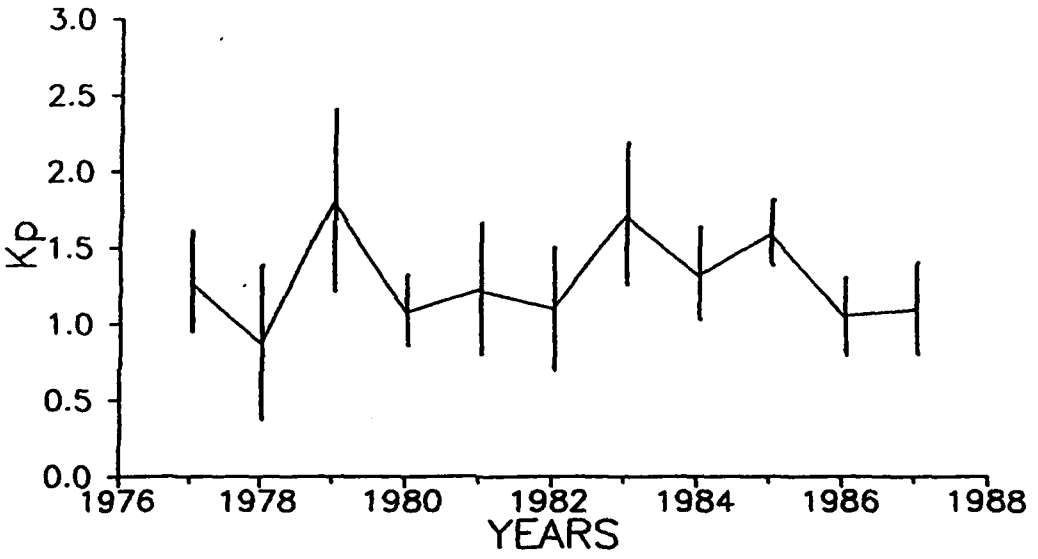

Fig. 8. Ten day average of January quiet time Kp index. Indices show no solar cycle variation. Error bars represent the standard deviation about the mean.

As discussed in Chapter II, the Richards-Torr ionospheric model is used in this investigation for determination of the variables α and ho, which are required for calculation of the meridional winds. The development of the Richards-Torr ionospheric model restricts its applicability to the mid-latitudes, which is the geographic region of concern for this investigation. As previously stated, this model incorporates seasonal, solar cycle, and diurnal variations. All of these variations come into play in the determination of the meridional neutral wind [Roble et al., 1977; Young et al., 1980]. Additionally, the Richards-Torr model is able to handle varying levels of geomagnetic activity. This is not a critical criteria in the present study as only quiet to moderate levels of geomagnetic activity ($Ap \leq 8$) are encountered.

By the use of a grid system, which consists of a longitudinal and latitudinal chain of ionosonde stations, as indicated in Figure 2, variations of the meridional wind with respect to location, universal time, and local time are studied. The timescale of this study provides a means of investigating the transition from solar maximum winds to solar minimum winds.

Data Analysis

As with most studies of this magnitude, two problem areas must be addressed. First, a reduction of the final results to a managable, but representative, level is es-

sential so as not to obscure their meaning. Second, a degree of statistical confidence is also required for the application of the results to be of use in future studies. Only the second problem area will be addressed at the present time as the manner of presentation of results will be dealt with in conjunction with the discussion of the results of this investigation.

Based on equation (1), one can establish the error, or uncertainty, in the calculated meridional winds as a function of time, α, ho, and hmax. By finite difference techniques, using the root mean square method, the uncertainty in U is given as:

$$\delta U = \left\{ \frac{1}{\alpha^2} \left[(\delta hmax)^2 + (\delta ho)^2 + \left(\frac{ho - hmax}{\alpha} \right)^2 (\delta\alpha)^2 \right] \right\}^{1/2} \quad (8)$$

or

$$\frac{\delta U}{U} = \frac{1}{ho - hmax} \left[(\delta hmax)^2 + (\delta ho)^2 + \left(\frac{ho - hmax}{\alpha} \right)^2 (\delta\alpha)^2 \right]^{1/2} \quad (9)$$

Determination of δho and $\delta\alpha$ are based on the evaluation of the method of calculation of α and ho by the Richards-Torr ionospheric model. For the value of δhmax, from the Bradley-Dudeney model, a value of ± 10 km is used in the present investigation [Bradley and Dudeney, 1973; Dudeney, 1983]. By a linear regression of α, as illustrated in Figure 9,

$$\delta\alpha = \sqrt{2}\, \frac{\delta h_{RT}}{u_2 - u_1} \quad (10)$$

By definition of ho,

$$ho = h_{RT1} + \frac{0 - u_1}{u_2 - u_1} (h_{RT2} - h_{RT1}) \quad (11)$$

then

$$\delta ho = \left[\left(\frac{u_2}{u_2 - u_1} \right)^2 (\delta h_{RT1})^2 + \left(\frac{u_1}{u_2 - u_1} \right)^2 (\delta h_{RT2})^2 \right]^{1/2} \quad (12)$$

In accordance with the model execution notes $\delta h_{RT1} = \delta h_{RT2} = \delta h_{RT} = \pm$ 10 km and by substitution

$$\delta ho = (\delta h_{RT}) \left[\frac{u_2^2 + u_1^2}{(u_2 - u_1)^2} \right]^{1/2} \quad (13)$$

The above error analysis is strictly a statistical error analysis and does not account for the fact that the model is, at best, an approximation to average conditions.

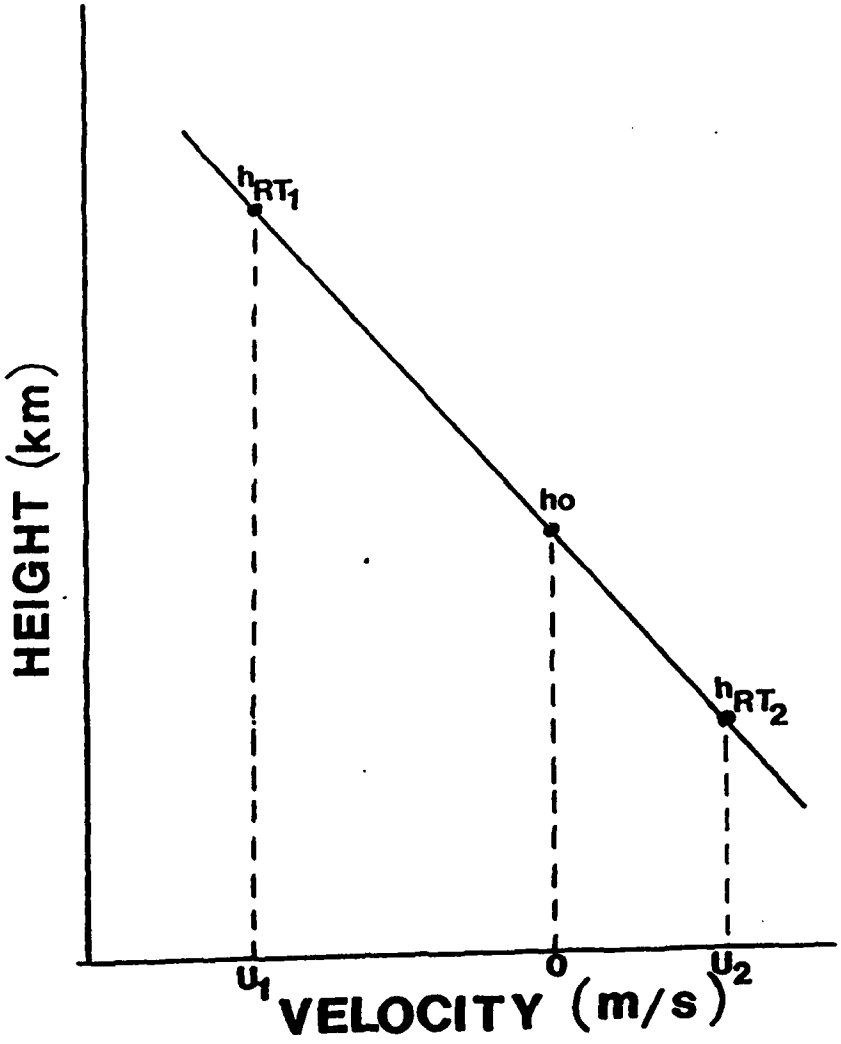

Fig. 9. Statistical error analysis of α and ho by linear reression techniques of the Richards-Torr ionospheric model.

CHAPTER IV

RESULTS AND DISCUSSION

Solar Cycle Variations

The major contributor to the mid-latitude circulation pattern is heating by absorption of solar UV and EUV radiation. The level and intensity of such radiation is directly proportional to the level of solar activity. Observation of sunspot numbers and the 10.7 cm solar radio flux, shown in Figure 10, provide a means of predicting ionospheric parameters, such as the F region critical frequency and peak layer height [Smith and King, 1981]. An increase in solar activity increases the horizontal pressure gradients, which is the main driver of the thermospheric winds. At the same time an increase in the charged particle population leads to increased ion drag, which inhibits the winds. In general, as the level of solar activity decreases, daytime, poleward wind speeds increase because ion drag decreases more rapidly than the pressure gradient force [Rishbeth, 1972; Babcock and Evans, 1979; Hedin and Mayr, 1987; Lakshimi et al., 1988].

In Figure 11 and Figure 12 the dashed lines represent calculated meridional winds for a 24-hour period based on the average conditions of the ten most quiet days, as recorded in Appendix B. The solid lines represent the statistical error as calculated at 3-hour intervals. The

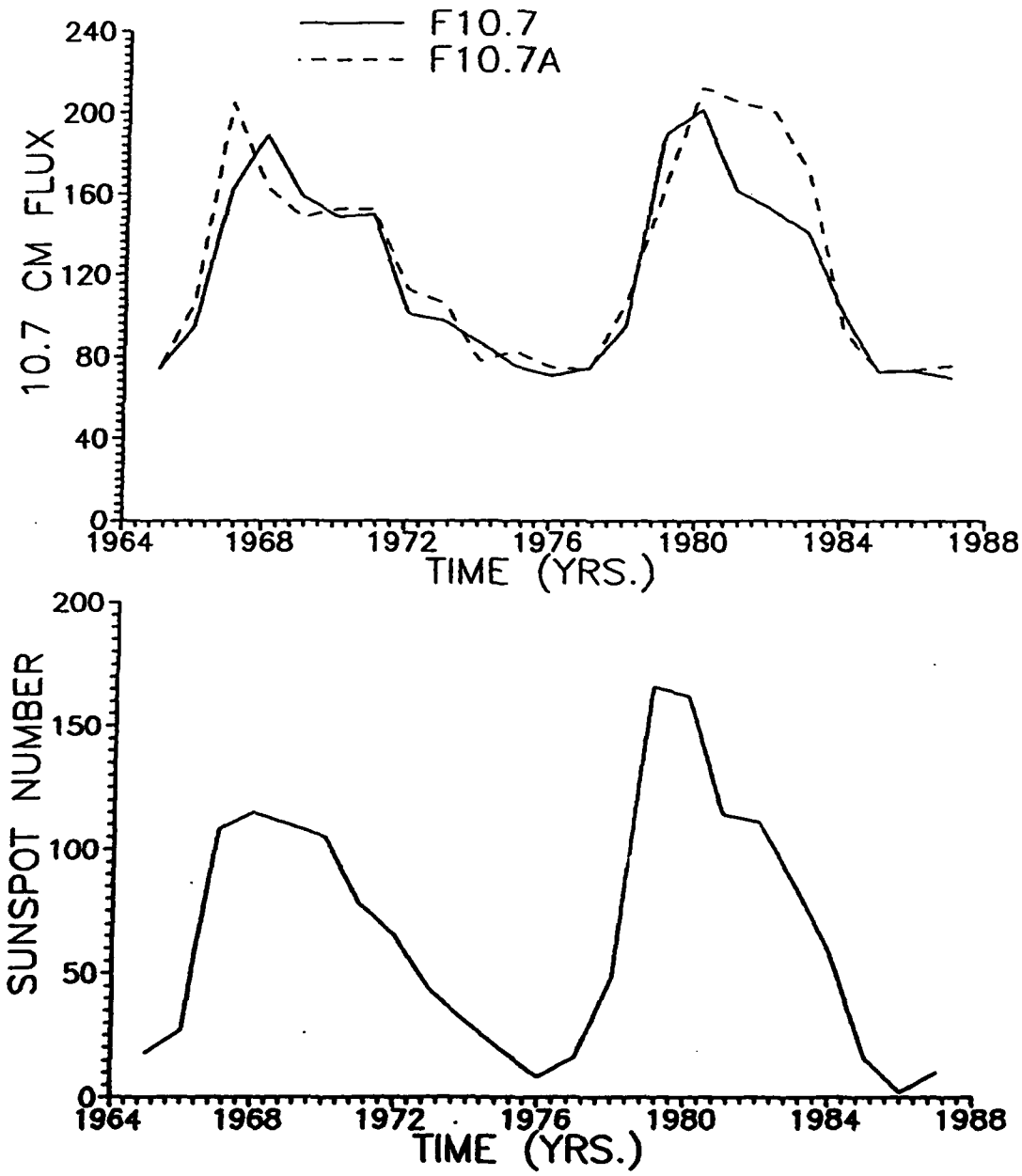

Fig. 10. Variations in the level of solar activity as seen in the 10.7 cm solar radio flux and mean sunspot number. Units of flux are 10^{-22} W m^{-2} Hz^{-1}.

decision to use a 3-hour interval representation is based on the fact that this investigation is primarily geared at studying large-scale cyclical trends of the meridional winds as opposed to looking at smaller scale phenomenon.

The results of this investigation indicate that the above statements are essentially correct. Figure 11 presents meridional winds for a chain of ionosonde stations which stretches from 43°S to 62°N geographic latitude and centered roughly at 140°E geographic longitude. In the case of the Northern Hemisphere stations of Akita and Khabarovsk, the poleward wind speeds (positive values) increase by roughly 30 m/s from solar maximum (1979) to solar minimum (1987) conditions. It is noted, however, that maximum poleward wind speeds are reached roughly three to four years prior to solar minimum and then level off. In the case of the higher latitude station of Yakutsk, an increase in poleward wind speeds of roughly 15 m/s is observed between 1979 and 1983. A gradual decline in the poleward wind then occurs. This result appears to be limited to this station alone and may be due in part to variations in the calculation of hmax by the IRI model ionosphere and that of the Bradley-Dudeney model. This point will be discussed in more detail in the error analysis section of this chapter.

Figure 12 presents meridional winds for a longitudinal chain of ionosonde stations centered at approximately 50°N geographic latitude. These stations also exhibit a 30 to 50

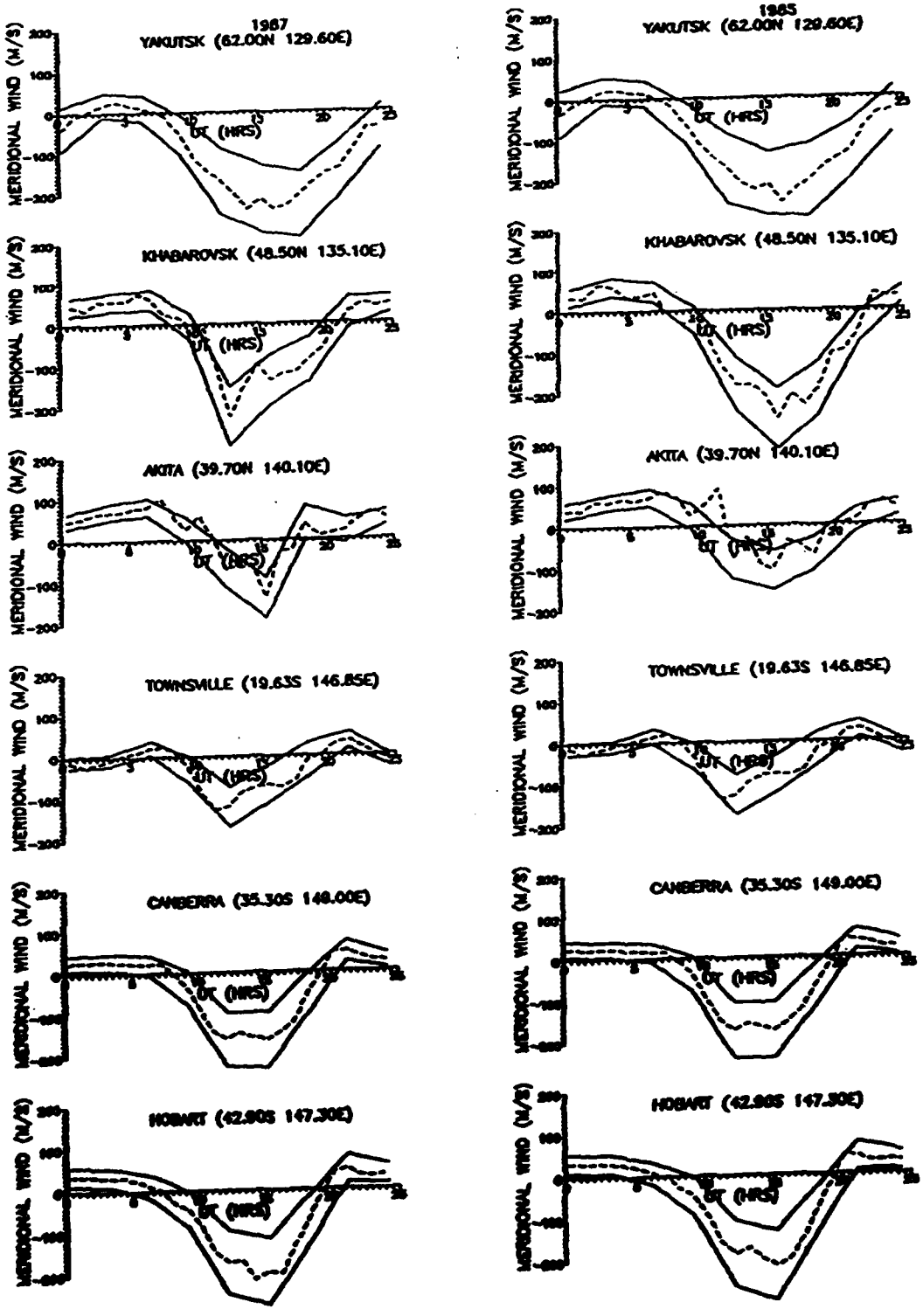

Fig. 11. Variations of the meridional wind for a latitudinal chain of ionosonde stations at 140°E longitude. Dashed lines represent calculated wind velocities and solid lines represent statistical uncertainties.

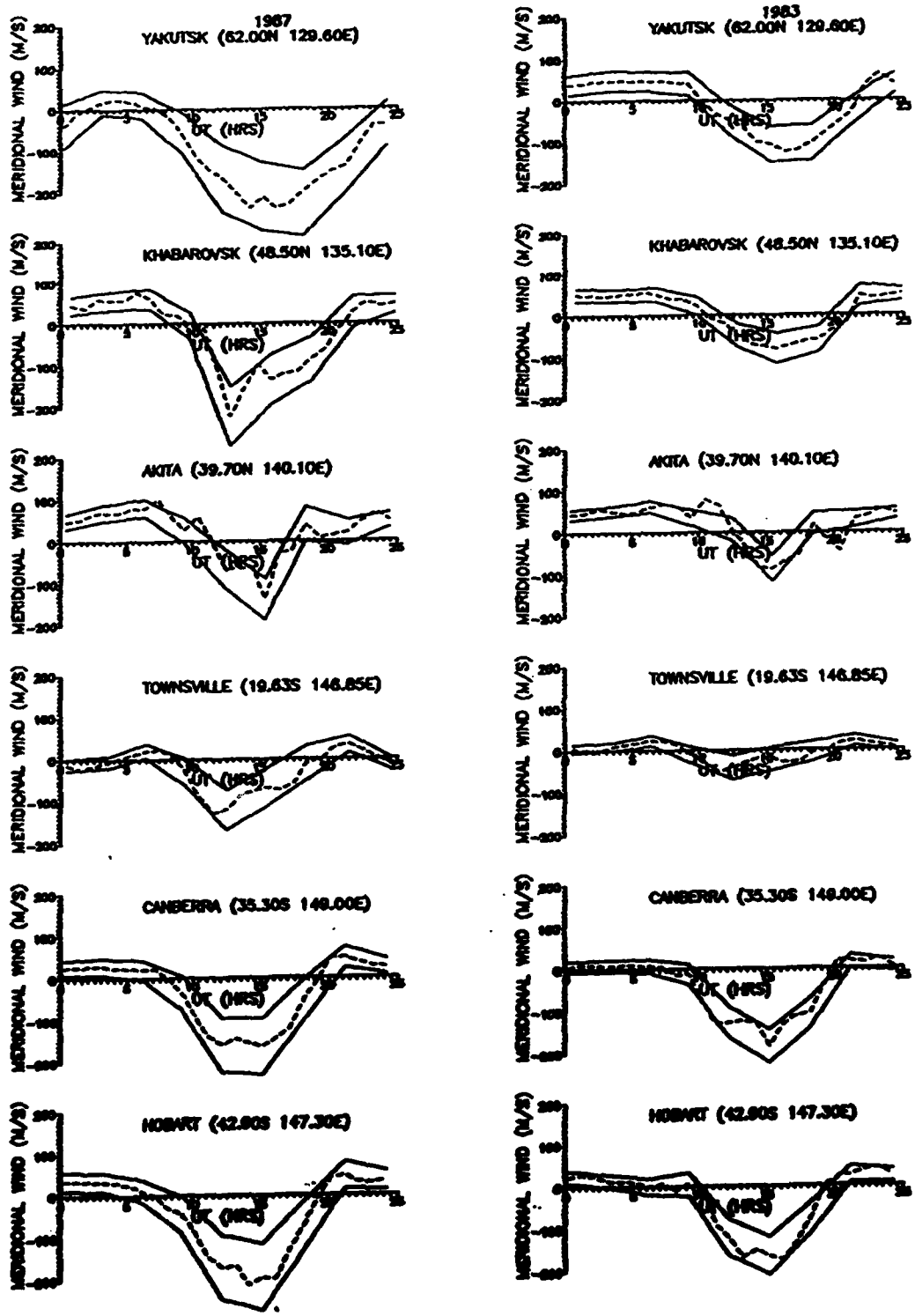

Figure 11 continued.

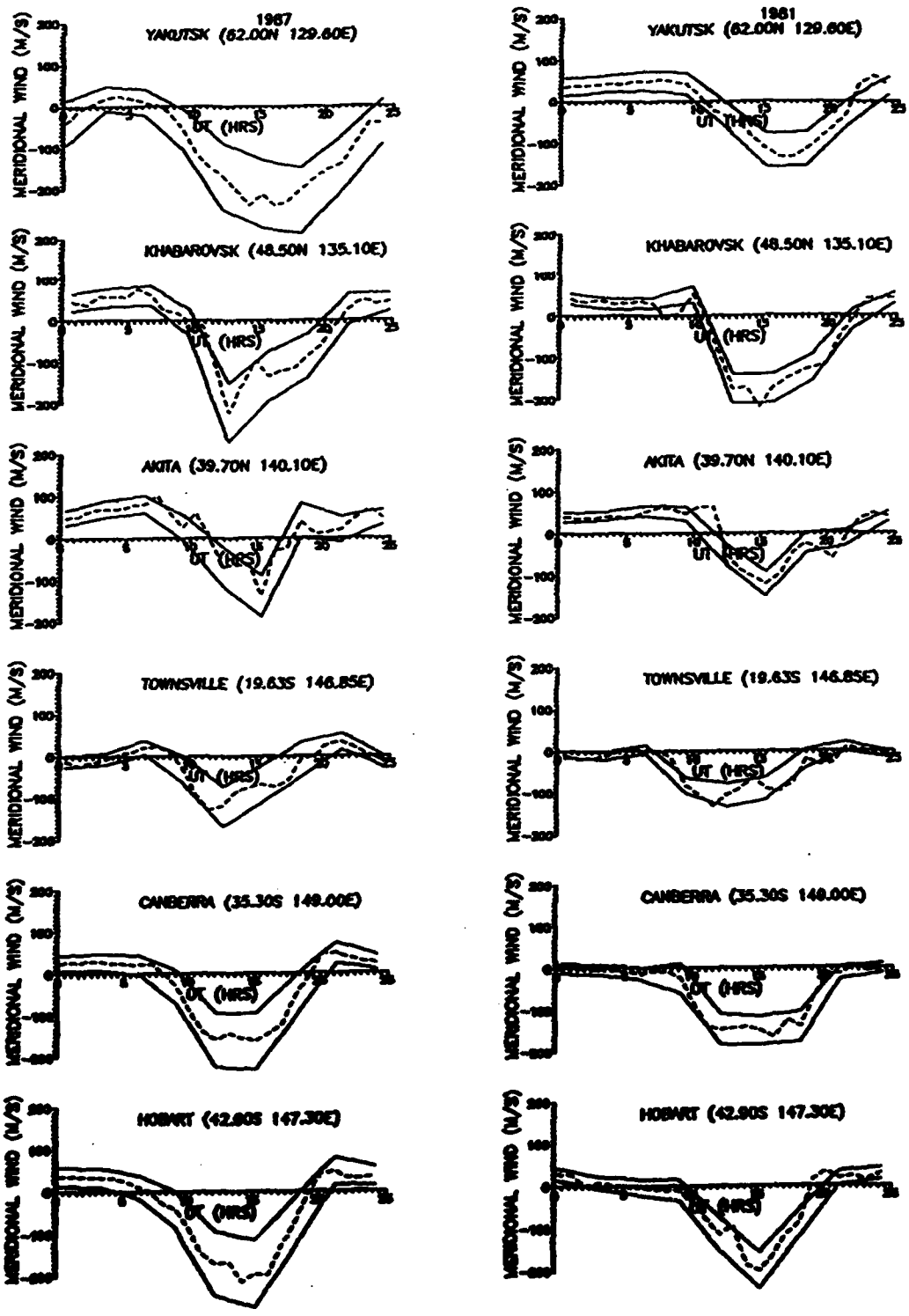

Figure 11 continued.

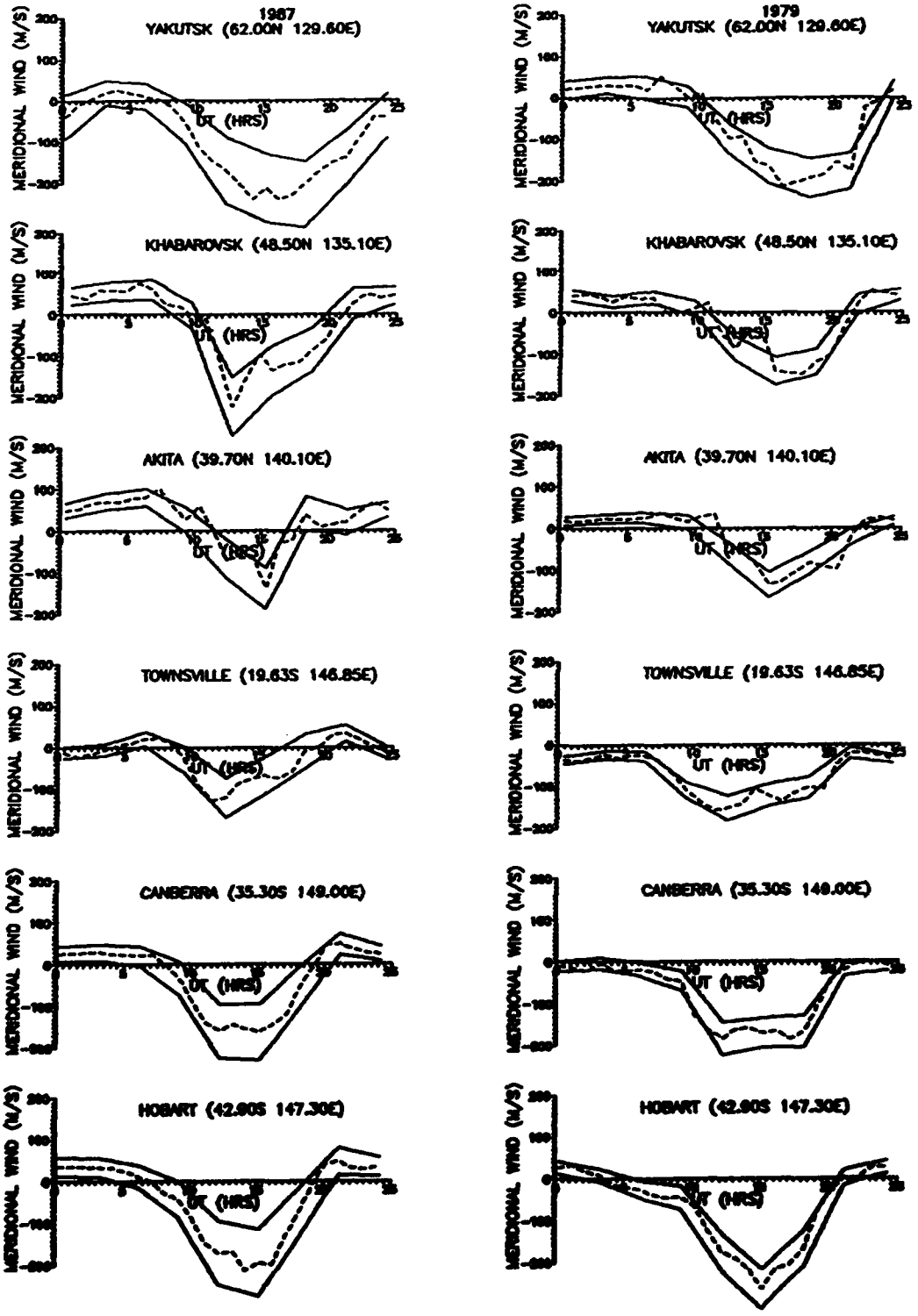

Figure 11 continued.

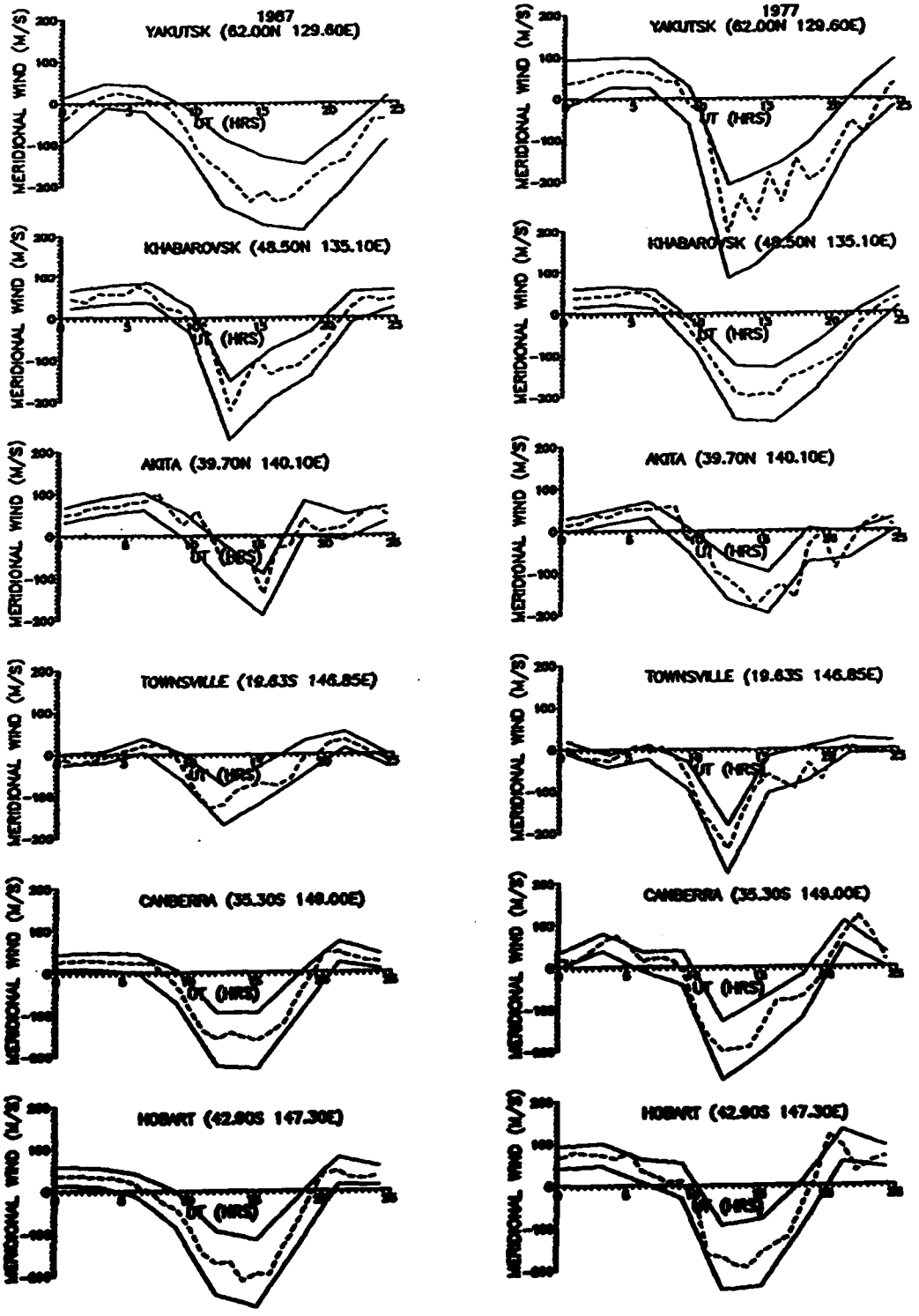

Figure 11 continued.

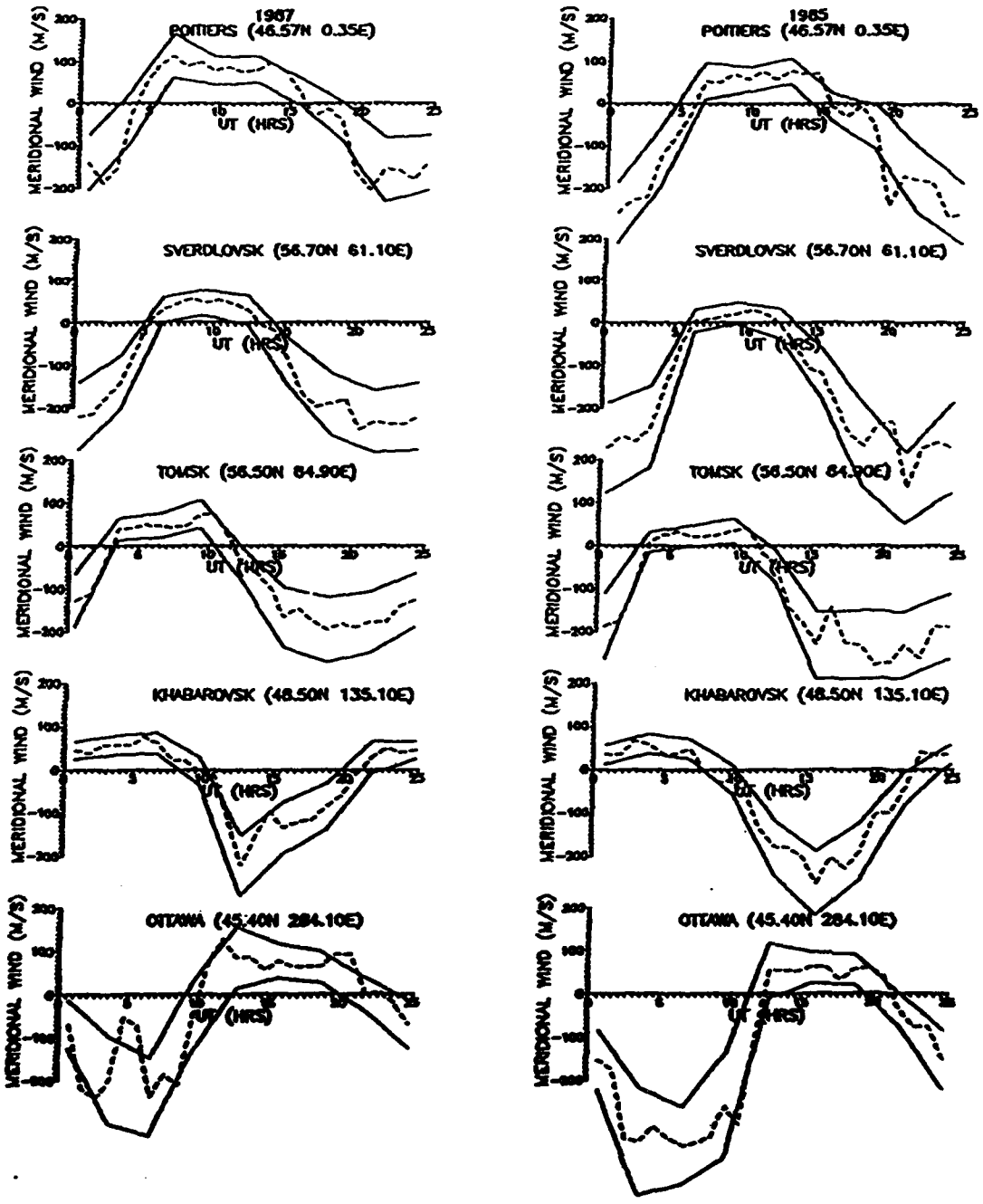

Fig. 12. Variation of the meridional winds for a longitudinal chain of ionosonde stations at 50°N latitude. Dashed lines represent calculated wind velocities and solid lines represent statistical uncertainties.

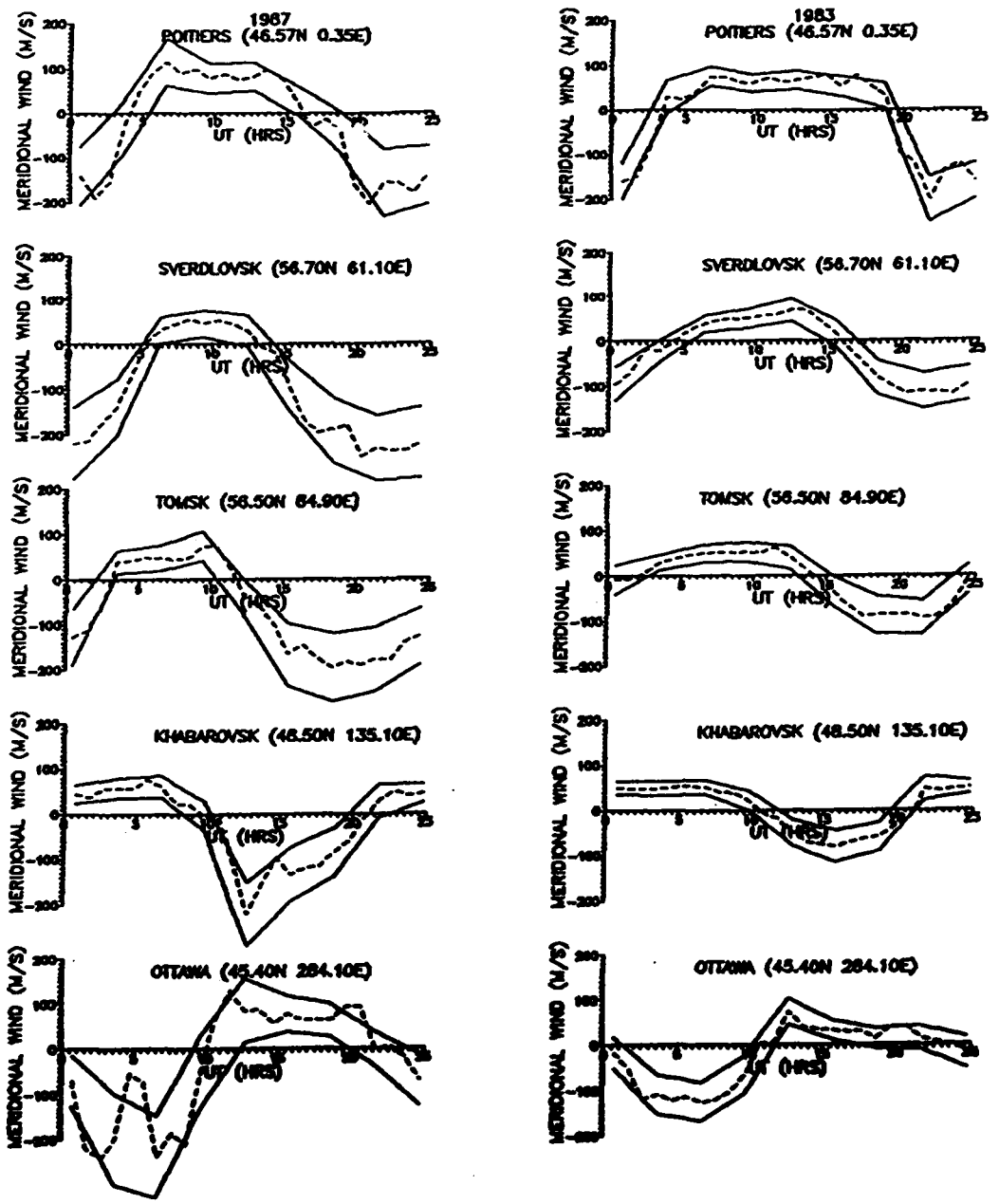

Figure 12 continued.

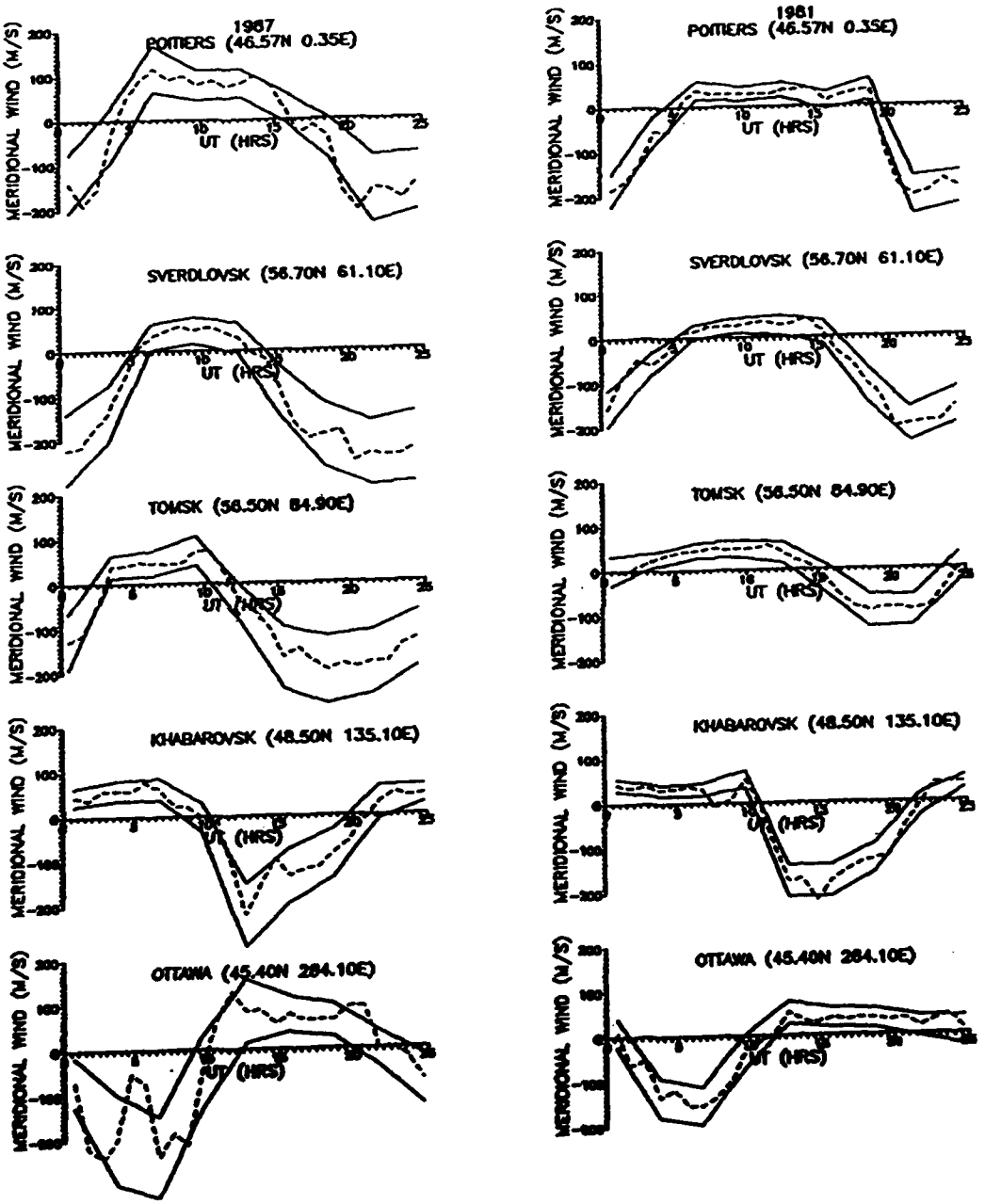

Figure 12 continued.

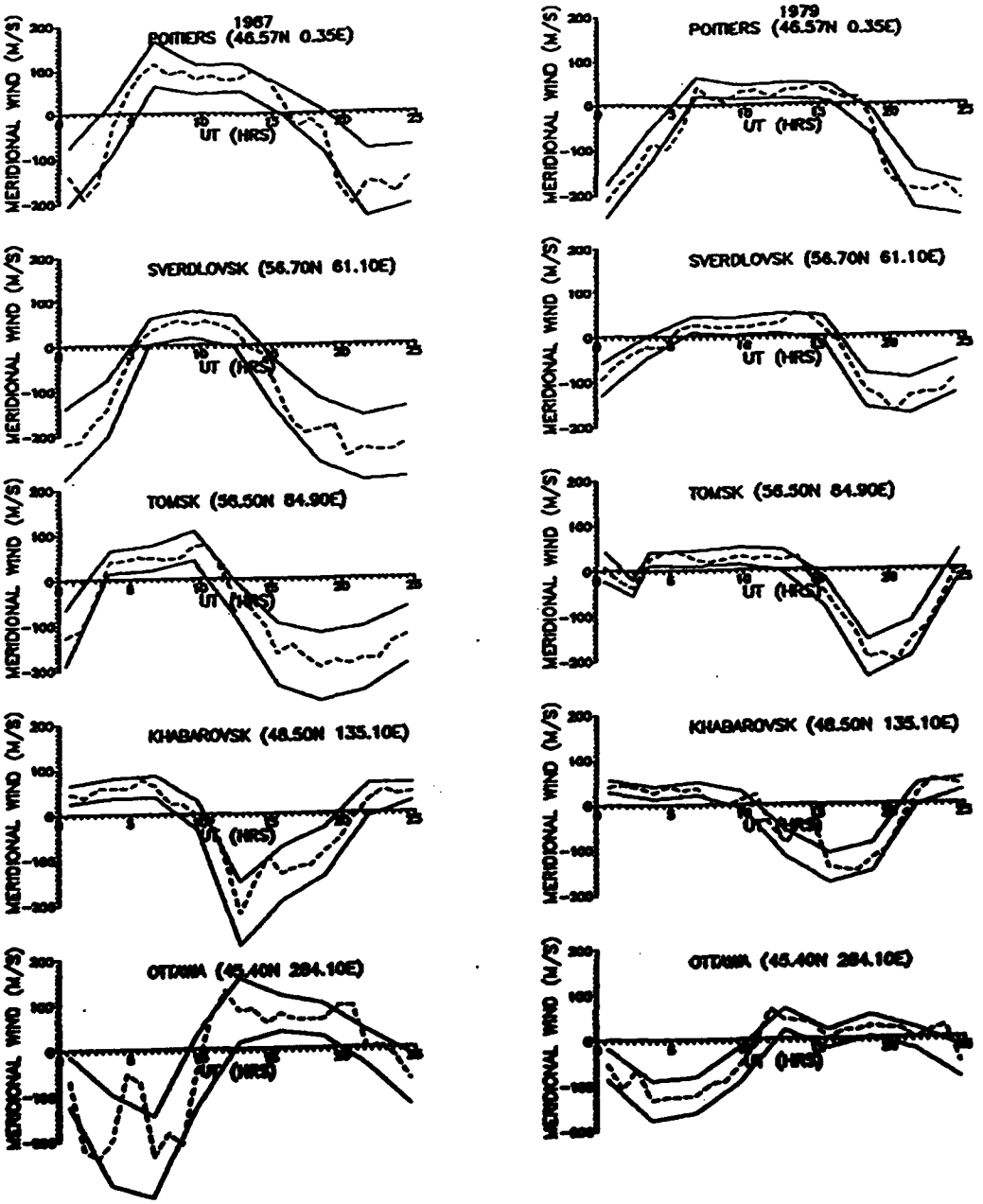

Figure 12 continued.

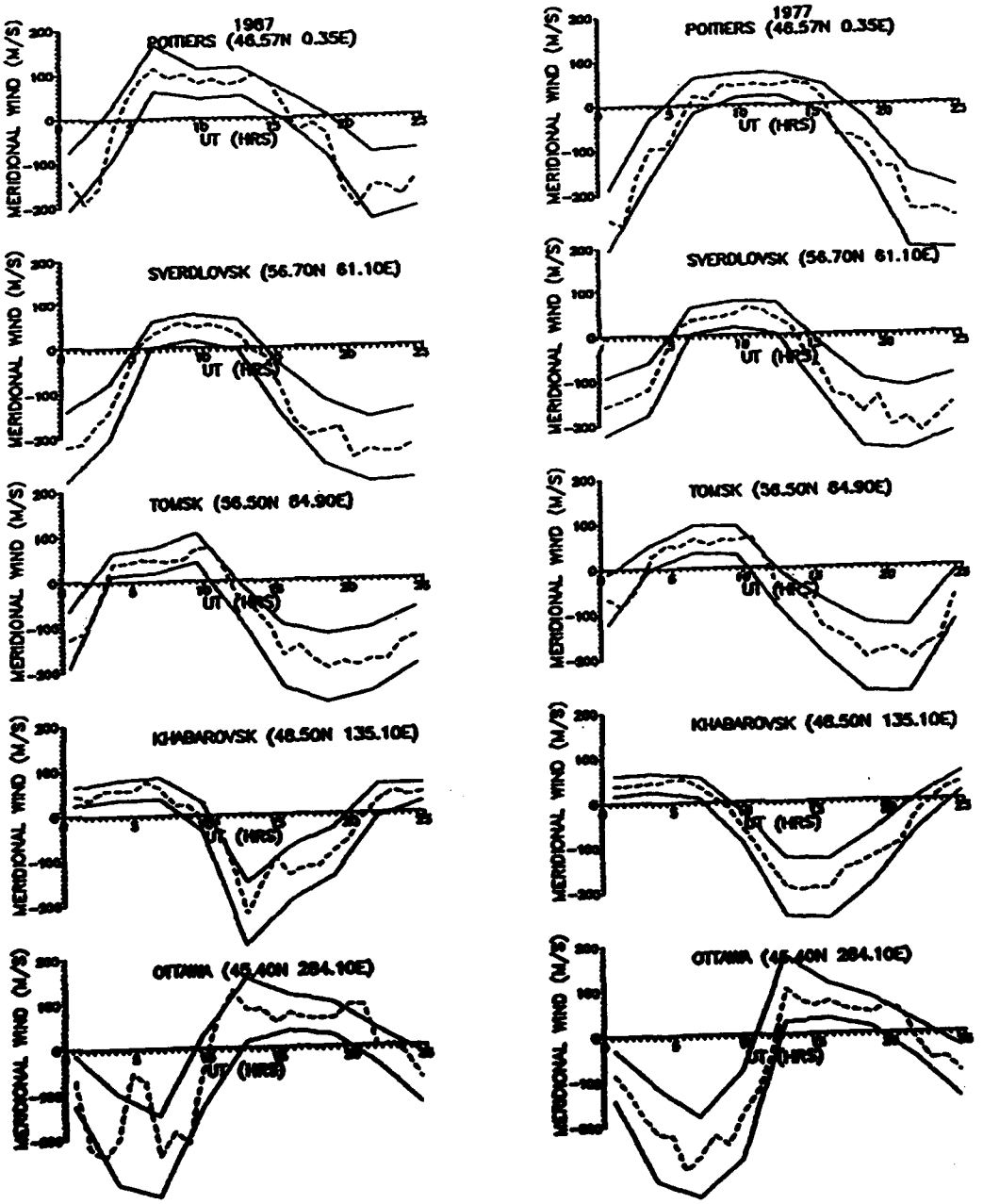

Figure 12 continued.

m/s increase in the speed of the poleward wind as time moves from solar maximum to solar minimum conditions. As a general rule, these stations also reach a maximum poleward wind speed three to four years prior to the time of solar minimum. This feature corresponds to a period of a slower rate of decline in the level of solar activity from solar maximum conditions to solar minimum conditions, as shown in Figure 10.

In the case of the Southern Hemisphere stations of Figure 11, the change in poleward wind speeds is not as apparent as has been noted for the northern stations. This is particularly true of the station of Townsville which is closer to the magnetic equator than the other stations of this investigation and may be subject to additional low latitude effects. Further discussion of this station will be deferred to the section on the repetitive nature of the meridional winds relative to the solar cycle, covering the period of 1965 to 1987. Poleward winds for the most southerly stations of Canberra and Hobart again demonstrate a general increase in wind speed with decreasing solar activity. The relative increase of these two stations is only 20 to 25 m/s and, as previously noted, the maximum speeds are reached roughly three to four years prior to solar minimum at 1987.

Corresponding to the period of rapid increase in solar activity, 1977 to 1979, there is a general decline in pole-

ward wind speeds of roughly 30 to 35 m/s for the Northern Hemisphere stations. A more drastic decline of approximately 40 m/s is noted in the most southern stations of Canberra and Hobart. The station of Townsville, located at low latitudes, is again the exception to this pattern.

As illustrated in Figure 11 and Figure 12, the change in the equatorial wind speed (negative values) of the meridional winds show a more drastic solar cycle dependence than the poleward winds. An overall pattern of slower wind speeds occurring at solar maximum and faster wind speeds at solar minimum is noted. However, the slowest wind speeds at all stations occurs midway through the solar cycle (1981 to 1983). In the case of the Northern Hemisphere stations, the winds speeds increase over a range of 70 to 160 m/s between the period of 1983 to that of solar minimum, at 1987. For the period of solar maximum, 1979, to the midway point, 1983, the meridional winds show a decrease over the range of 40 to 130 m/s. The period of slowest equatorial wind speeds corresponds to the time frame where the slope of the decline in both the 10.7 cm solar radio flux and sunspot number decrease, as seen in Figure 10. The Southern Hemisphere stations, with the exception of Canberra, show a similar pattern with the slowest equatorial winds occurring midway through the solar cycle. In the case of Hobart and Townsville a range of increase in the wind speeds of 70 to 120 m/s is detected for the period of 1983 to 1987. The

period of solar maximum to midway through the cycle, indicate an overall decrease over the range of 100 to 150 m/s. The station of Canberra exhibits a difference of approximately 25 m/s between both periods of solar maximum and solar minimum versus wind speeds calculated at the midway period of the solar cycle.

A notable difference in the pattern of the meridional winds at solar maximum versus those found at solar minimum is the duration of the equatorial winds. As seen in Figure 11, this variation is most noticeable in the Southern Hemisphere stations where the winds blow in an equatorial direction for approximately 15 to 20 hours at solar maximum and only 9 to 11 hours at solar minimum. This result corresponds to the work of Babcock and Evans [1979] for Millstone Hill. This result may in part be attributed to the difference in auroral forcing and is manifested in the summer to winter interhemisphere flow regime [Roble, et al., 1977].

Repetitive Nature of the Meridional Winds

With the exception of Townsville, all other stations exhibit a diurnal fluctuation in the critical ionosonde frequency, foF2, and in the associated F2 peak layer height [Amaycenc, 1974; Forbes and Garrett, 1976]. This variation is illustrated in Figure 13, which provides a representation of the variability of the critical ionosonde frequency foF2

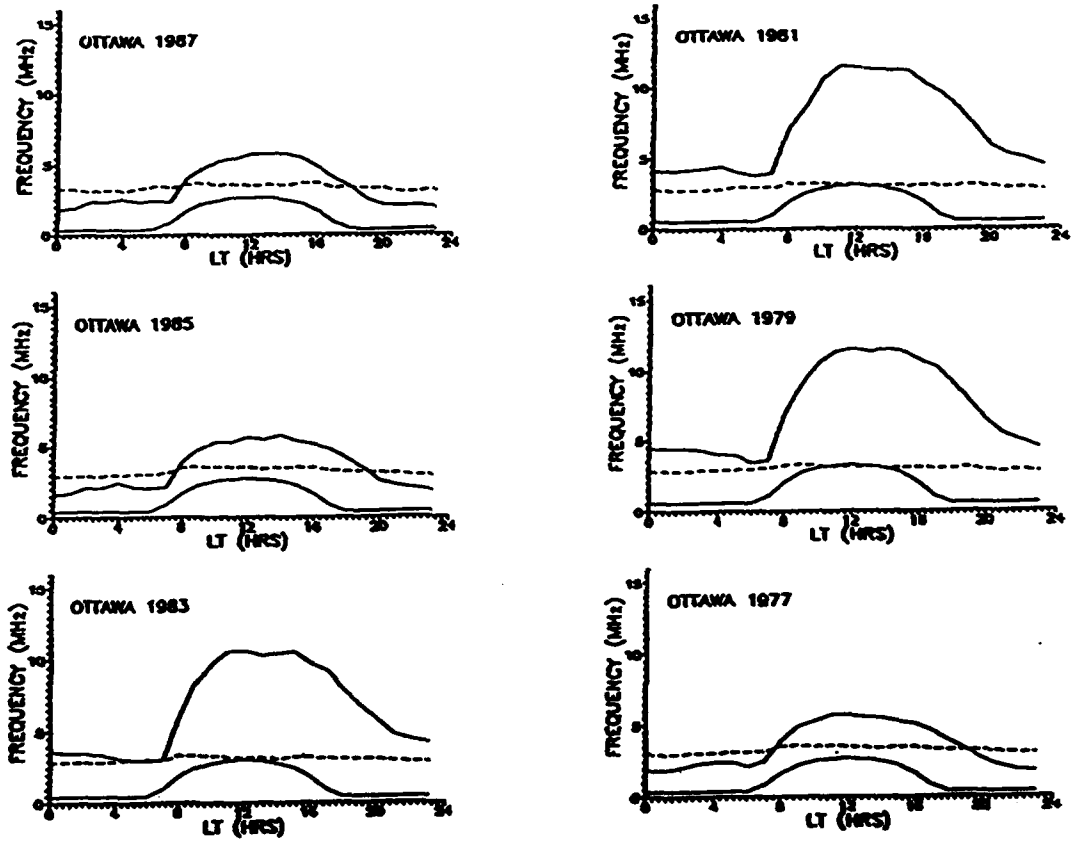

Fig. 13. Representative diurnal variation in the critical frequencies, foF2 and foE, and M(3000)F2 throughout the solar cycle. Solid lines represent foF2 and foE and dashed lines represent M(3000)F2.

throughout a solar cycle. Comparison of the critical frequencies, foF2 and foE, along with the transmission factor M(3000)F2, and the solar indices for the cycle of 1965 to 1976 to that of the cycle of 1977 to 1987 indicate a high degree of similarity. Within the limits of uncertainty of the present method of determining the magnitude of the meridional winds, one would expect similar patterns and solar cycle variations for the earlier cycle as have been detected in the 1977 to 1987 cycle.

As seen in Figure 14, Townsville exhibits a semidiurnal variation in the ionosonde parameter of foF2. This variation is subsequently reflected in the values of hmax and ultimately in the magnitude of the meridional winds [Harper, 1973; Hong and Lindzen, 1976; Harper, 1979; Mayr et al., 1979; Burnside et al., 1983]. Figure 15 illustrates the semidiurnal nature of the meridional winds as well as their repetitive solar cycle variations over the period of two solar cycles. As has been discussed previously, both the equatorward and poleward wind speeds increase with decreasing solar activity. The magnitude of these variations is less than for those stations which are more distant from the magnetic equator. This is most likely due to a need to account for the $\mathbf{E} \times \mathbf{B}$ zonal wind field, wave propagation effects from below, and perhaps due to the existence of a more complex pressure gradient effect [Harper 1973; Harper, 1979; Mayr et al., 1979; Forbes, 1982]. Additional-

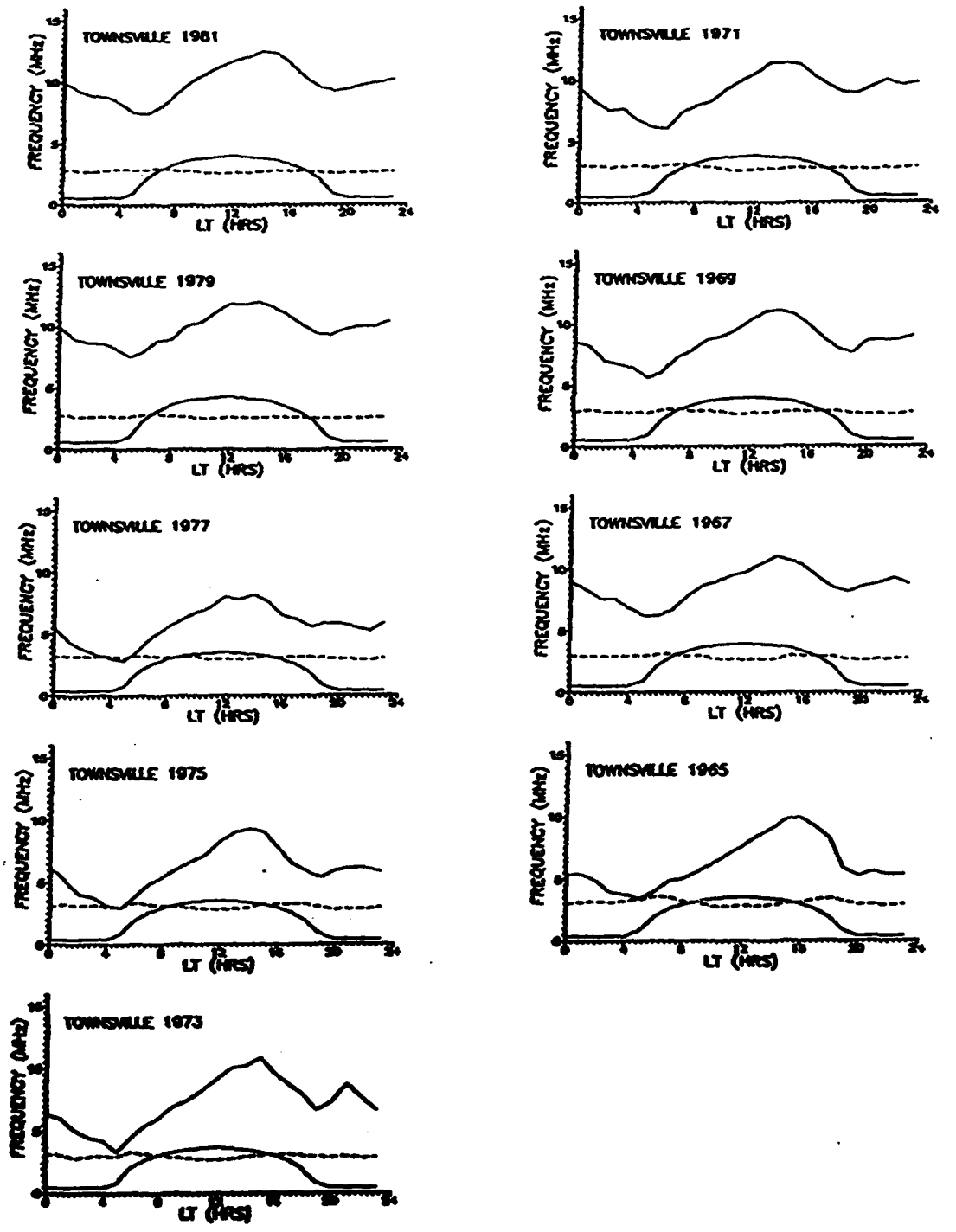

Fig. 14. Semi-diurnal variation of the critical frequencies, foF2 and foE, and M(3000)F2 for Townsville throughout the solar cycle. Solid lines represent foF2 and foE and dashed lines represent M(3000)F2.

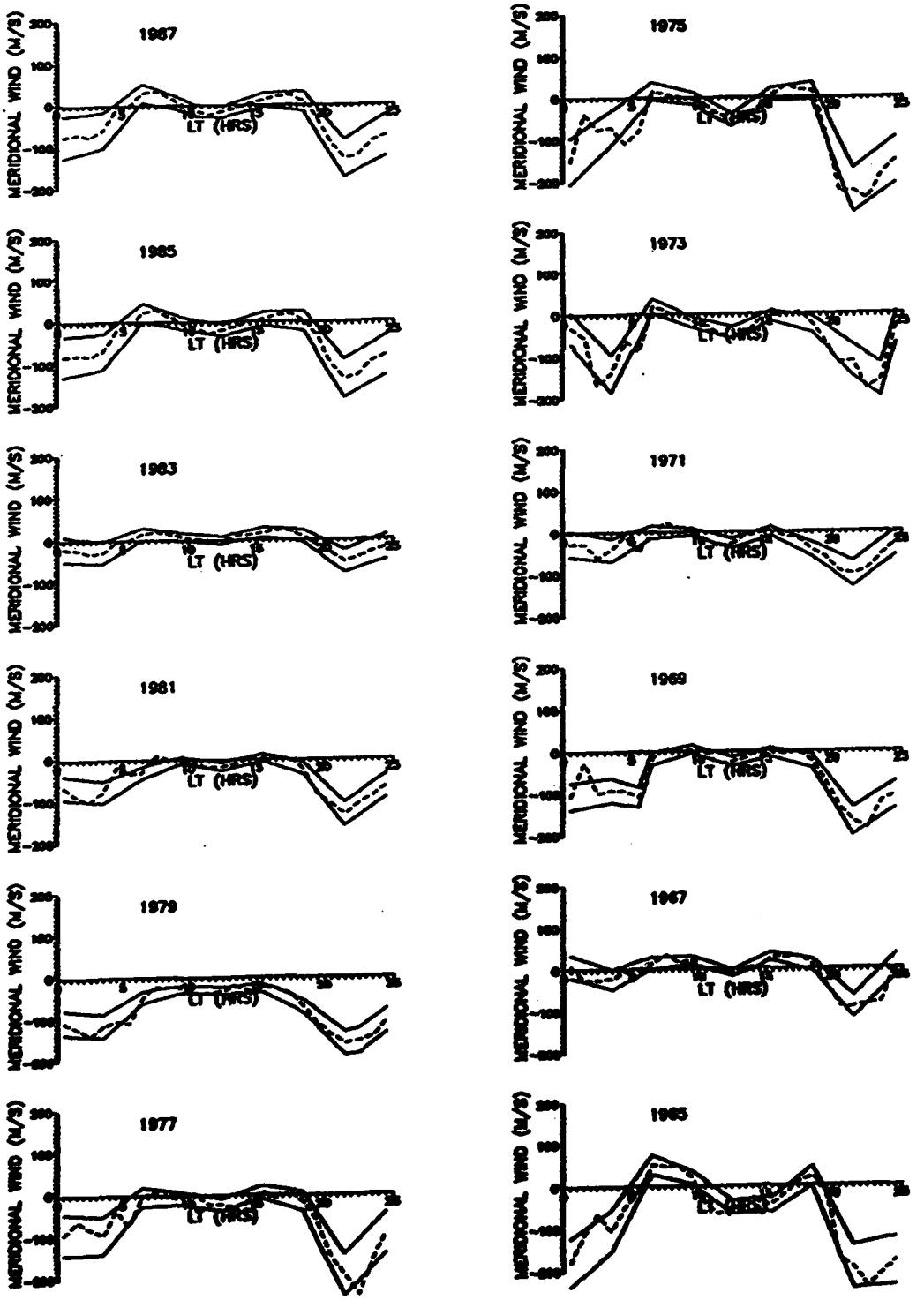

Figure 15. Semi-diurnal nature of the winds at Townsville and their repetitive nature for a period of two solar cycles.

ly, the slowest equatorward winds coincide with the periods of a change in the slope of the solar flux (1969 to 1971, and 1981 to 1983) and sunspot numbers, as was previouly discussed. The duration of the equatorward winds solar maximum also exceeds that found at solar minimum.

Error Analysis

Statistical uncertainties as described in Chapter III are accounted for in the prior discussion on solar cycle effects. The nighttime equatorward winds exhibit the highest level of uncertainty due to the effect of the α^{-2} dependency, as seen in the third term of equation (9), combined with the larger difference in ho and hmax for this time period.

Global wind patterns derived from ionosonde critical frequencies and IRI model parameters are similar in nature. One of the parameters provided by the IRI model is hmF2, as determined by an empirical fit of ionosonde data of foE, foF2, and M(3000)F2. These are the same parameters used in the Bradley-Dudeney model employed in this study of the meridional winds. Results of both models are valid only at mid-latitude regions. The results of this study agree with the findings of the study of Miller et al. [1989] in that differences between the IRI values of hmF2 and the Bradley-Dudeney model are most likely the result of local phenomena in terms of ionosonde data. Such transient behavior is too rapid to be adequately described by these empirical models.

Differences in these two models is most noticeable in the calculation of nighttime equatorial winds. These differences do not change the findings of this investigation as IRI calculated nighttime winds generally exceed the Bradley-Dudeney values at solar minimum. This would tend to increase the magnitude of the wind speeds at this time of the solar cycle. The difference in hmF2 is reversed at solar maximum with the Bradley-Dudeney values of hmax exceeding the IRI model values. This would tend to reduce the calculated wind speeds and lead to an even greater variation of the meridional winds throughout the solar cycle.

CHAPTER V

CONCLUSIONS AND RECOMMENDATIONS

At mid-latitudes, absorption of UV and EUV radiation are two of the principle ionization and heating sources within the thermosphere. The level of such radiation is directly related to the amount and intensity of solar activity. As with temperature variations, which create horizontal pressure gradients, which are the major driving force of mid-latitude thermospheric winds, there is a definite solar cycle dependence on the magnitude and direction of the meridional neutral winds. Use of ionosonde data provides a valuable means of calculating the magnitude and direction of the global scale variations of the these winds.

An increase in solar activity increases the pressure gradients, which drive thermospheric winds, but, at the same time, an increase in the charged particle population leads to an increased ion drag, which inhibits the winds. In general, as the level of solar activity decreases, daytime wind speeds increase because ion drag decreases more rapidly than the pressure gradient force. One area of future study in this area would be the investigation of the effect of combined auroral forcing and solar forcing on the mid-latitude thermospheric winds. This type of study would provide a much needed link between mid- and high latitude ionospheric models. A similar study could also be conducted

at low latitudes in order to complete a truly global ionospheric model of thermospheric circulation. At present the computer cost and time requirements may be prohibitive of such a large scale study.

For the slow declining phase of the solar cycle, this study indicates that for the Northern Hemisphere, as the level of solar activity decreases the poleward wind speeds increase by 30 to 50 m/s. This statement is illustrated in Figure 16 which provides a representation of the peak equatorward wind and poleward winds relative to the 10.7 cm solar radio flux. As a general rule, the poleward winds reach a near maximum velocity roughly three to four years prior to solar minimum and then level off until solar minimum occurs. This result varies, to some degree, from station to station, as seen in the case of Poitiers as illustrated in Figure 16. In the case of Southern Hemisphere stations, a less dramatic increase in poleward wind speeds with decreasing solar activity is observed. For the Southern Hemisphere locations, results of this study indicate a 20 m/s increase in the poleward wind speed is achieved three to four years prior to solar minimum.

In the rapidly increasing phase of the solar cycle, 1977 to 1979, a 30 m/s decrease in poleward winds occurs in the Northern Hemisphere, as illustrated in Figure 16. Mid-latitude stations in the Southern Hemisphere exhibit a 40 m/s decrease in the poleward wind.

As seen in Figure 16, the equatorial winds exhibit the same general pattern, as seen in poleward winds, with the faster speeds occurring at solar minimum and slower wind speeds occurring at solar maximum. However, a variation in this pattern is noted in that the slowest equatorial wind speeds generally occur midway through the cycle. This corresponds to a decrease in the rate of the 10.7 cm solar radio flux and sunspot number. Further research into this particular phenomenon is warranted. Additionally, in the Southern Hemisphere the duration of the equatorial winds also exhibits a solar cycle dependence in that the duration of the equatorial wind increases with increasing solar activity due to increased auroral forcing. Additional research into the relative importance of auroral forcing versus solar forcing of the mid-latitude thermospheric wind is required to explain this circulation phenomena more completely.

The results of this study indicate a definite trend in the winter solstice, meridional winds which correlates to the 11-year solar cycle. In the case of poleward, meridional winds, a direct correlation has been observed as the faster wind speeds occur at solar minimum and slower wind speeds occur at solar maximum. For the equatorial winds, an offset is observed in that the faster wind speeds occur at solar maximum and minimum while the slowest wind speeds occur midway through the cycle. Such results have a

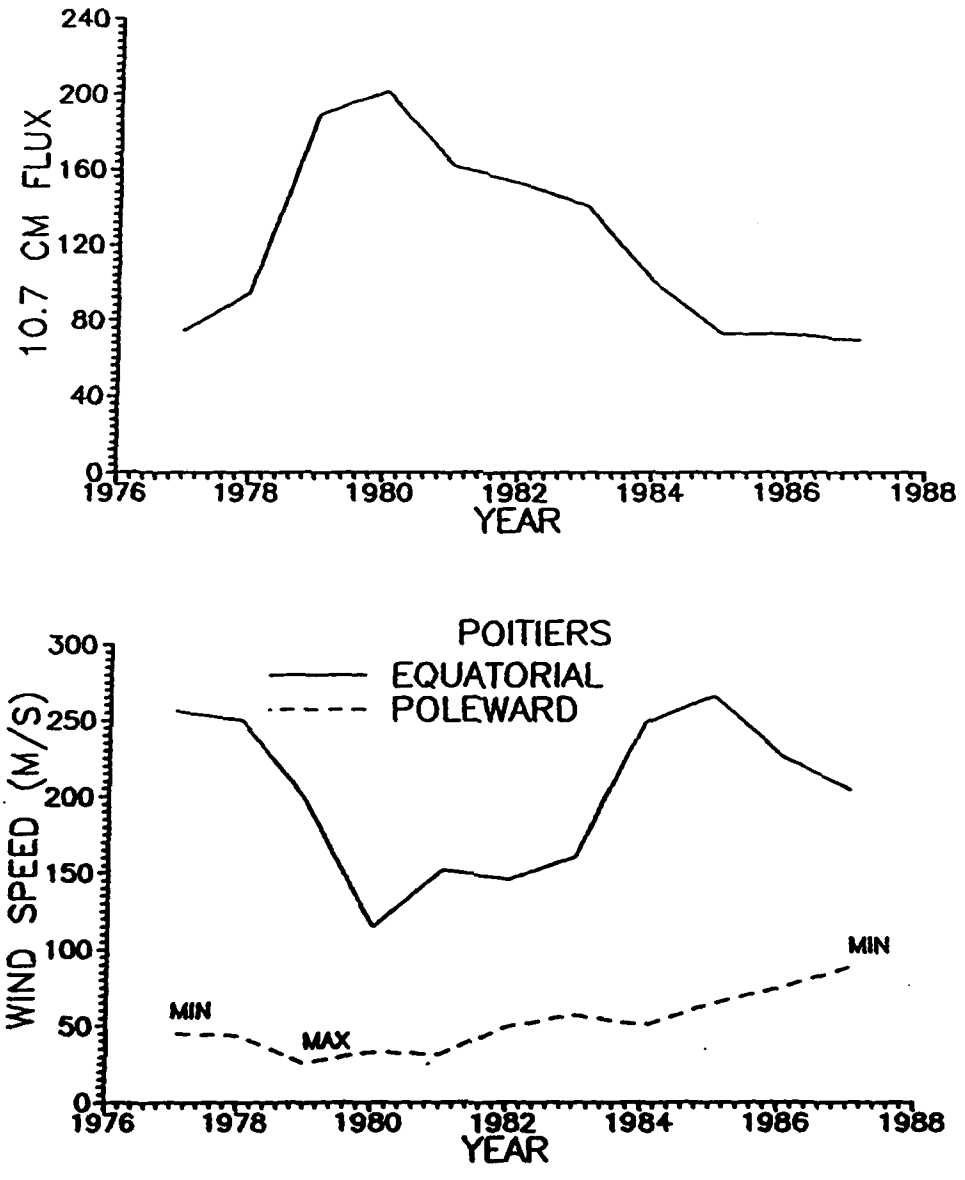

Fig. 16. Variation of the equatorial (nighttime) and poleward (daytime) meridional winds for one solar cycle relative to the 10.7 cm solar radio flux. Units of flux are 10^{-22} W m^{-2} Hz^{-1}.

bearing on mid-latitude plasma transports phenomenon.

Statistical uncertainties are largest in the nighttime, equatorward winds due to the effect of the α^{-2} dependency as seen in the third term of equation (9) of Chapter II. The size of the uncertainty is enhanced by the greater difference in ho and hmax for this time period.

Additional areas of study in this area of thermospheric circulation might include:

1) A study of 22-year cycle effects,

2) A comparison of the variability of thermospheric winds with solar flare activity throughout the solar cycle, and

3) Development of and incorporation of a wind model for the current mid-latitude ionospheric models to incorporate ionosonde, radar, or satellite data, which are required for such calculations.

REFERENCES

Amayenc, P., Tidal Oscillations of the Meridional Neutral Wind at Midlatitudes, Radio Sci., 9, 281-293, 1974.

Babcock, R. R. Jr., and J. V. Evans, Seasonal and Solar Cycle Variations in the Thermospheric Circulation Observed Over Millstone Hill, J. Geophys. Res., 84, 7348-7352, 1979.

Baird, D. C., An Introduction to Measurement Theory and Experiment Design, Prentice-Hall, Inc., New Jersey, 1962.

Banks, P. M., and G. Kockarts, Aeronomy: Part A, Academic Press, New York, 1973.

Blum, P. W., and I. Harris, The Global Wind System in the Thermosphere, Space Res. XIII, Vol. 1, Akademie-Verlag, 369-375, 1973.

Bradley, P. A., and J. R. Dudeney, A Simple Model of the Vertical Distribution of Electron Concentration in the Ionosphere, J. Atmos. Terr. Phys., 35, 2131-2146, 1973.

Burnside, R. G., R. A. Behnke, and J. C. G. Walker, Meridional Neutral Winds in the Thermosphere at Arecibo: Simultaneous Incoherent Scatter and Airglow Observations, J. Geophys. Res., 88, 3181-3189, 1983.

Challinor, R. A., and D. Eccles, Longitudinal Variations of the Mid-latitude Ionosphere Produced by Neutral-Air Winds I. Neutral-Air Winds and Ionospheric Drifts in the Northern and Southern Hemispheres, J. Atmos. Terr. Phys., 33, 363-369, 1971.

Chen, F. F., Introduction to Plasma Physics and Controlled Fusion, Vol. 1, 2nd edition, Plenum Press, New York, 1984.

Chernosky, E. J., P. F. Fougere, R. O. Hutchinson, The Geomagnetic Field, In Shea L. Valley (Ed.), Handbook of Geophysics and Space Environments, Air Force Cambridge Research Laboratories, 11.1-11.61, 1965.

Conkright, R. O., and H. I. Brophy, Catalog of Ionosphere Vertical Soundings Data, NOAA Report, UAG-85, 1982.

Dickinson, R. E., E. C. Ridley, and R. G. Roble, Meridional Circulation in the Thermosphere II. Solstice Conditions, J. Atmos. Sci., 34, 178-192, 1977.

Dudeney, J. R., The Accuracy of Simple Methods for Determining the Height of the Maximum Electron Concentration of the F2 Layer from Scaled Ionospheric Characteristics, J. Atmos. Terr. Phys., 45, 629-640, 1983.

Forbes, J. M., and H. B. Garrett, Solar Diurnal Tide in the Thermosphere, J. Atmos. Sci., 33, 2226-2241, 1976.

Forbes, J., Atmospheric Tides 2. The Solar and Lunar Semidiurnal Components, J. Geophys. Res., 87, 5241-5252, 1982.

Hanson, W. B., and T. N. L. Patterson, The Maintenance of the Nighttime F-Layer, Planet. Space Sci., 12, 979-997, 1964.

Harper, R. M., Nighttime Meridional Neutral Winds Near 350 km at Low to Mid-latitudes, J. Atmos. Terr. Phys., 35, 2023-2034, 1973.

Harper, R. M., A Semidiurnal Tide in the Meridional Winds at F Region Heights in the Low Latitudes, J. Geophys. Res., 84, 411-415, 1979.

Hedin, A. E., A Revised Thermospheric Model Based on Mass Spectrometer and Incoherent Scatter Data: MSIS-83, J. Geophys. Res., 88, 10,170-10,180, 1983.

Hedin, A. E., and H. G. Mayr, Solar EUV Induced Variations in the Thermosphere, J. Geophys. Res., 92, 869-875, 1987.

Hernandez, G., and R. G. Roble, Direct Measurement of Nighttime Thermospheric Winds and Temperatures 1. Seasonal Variations During Geomagnetic Quiet Periods, J. Geophys. Res., 81, 2065-2074, 1976.

Hernandez, G., and R. G. Roble, Direct Measurements of the Nighttime Thermospheric Winds and Temperatures 3. Monthly Variations During Solar Minimum, J. Geophys. Res., 82, 5505-5511, 1977.

Hernandez, G., Mid-latitude Thermospheric Neutral Kinetic Temperatures 1. Solar, Geomagnetic, and Long Term Effects, J. Geophys. Res., 87, 1623-1632, 1982.

Herraro, F. A., H. G. Mayr, and N. W. Spencer, Low Latitude Thermospheric Meridional Winds Between 250 and 450 km Altitude: AE-E Satellite Data, J. Atmos. Terr. Phys., 50, 1001-1006, 1988.

Hong, S., and R. S. Lindzen, Solar Semidiurnal Tide in the Thermosphere, J. Atmos. Sci., 33, 135-153, 1976.

Jacchia, L. G., and J. W. Slowey, A Study of the Variations in the Thermosphere Related to Solar Activity, Space Res. XIII, Vol 1., Akademie-Verlag, 343-348, 1973.

Lakshimi, D. R., B. M. Reddy, and R. S. Dabas, On the Possible Uses of EUV Data for Ionospheric Predictions, J. Atmos. Terr. Phys., 50, 207-213, 1988.

Mayr, H. G., and I. Harris, Some Characteristics of Electric Field Momentum Coupling with the Neutral Atmosphere, J. Geophys. Res., 83, 3327-3336, 1978.

Mayr, H. G., and I. Harris, F - Region Dynamics, Rev. Geophys. Space Phys., 17, 492-510, 1979.

Mayr, H. G., I. Harris, N. W. Spencer, A. E. Hedin, L. E. Wharton, H. S. Porter, J. C. G. Walker, and H. C. Carlson Jr., Tides and the Midnight Temperature Anomaly in the Thermosphere, Geophys. Res. Lett., 6, 447-450, 1979.

Miller, K. L., D. G. Torr, and P. G. Richards, Meridional Winds in the Thermosphere Derived From Measurement of the F2 Layer Height, J. Geophys. Res., 91, 4531-4535, 1986.

Miller, K. L., J. E. Salah, and D. G. Torr, The Effects of Electric Fields on Measurements of the Meridional Neutral Winds in the Thermosphere, Annales Geophysicae, 5, 337-342, 1987.

Miller, K. L., and D. G. Torr, A Global Study of the Meridional Winds in the Thermosphere, Adv. Space Res., 7, 10,299-10,302, 1987.

Miller, K. L., A. E. Hedin, P. J. Wilkinson, D. G. Torr, and P. G. Richards, Neutral Winds Derived From IRI Parameters and From HWM87 Wind Model for the SUNDIAL Campaign of September 1986, Adv. Space Res., (In Press), 1989.

Rishbeth, H., F2 Layer Rates at Sunspot Minimum, J. Atmos. Terr. Phys., 28, 911-918, 1966.

Rishbeth, H. Thermospheric Winds and the F-Region: A Review, J. Atmos. Terr. Phys., 34, 1-47, 1972.

Roble, R. G., and R. E. Dickinson, The Effects of Displaced Geomagnetic and Geographic Poles on the Thermospheric Neutral Winds, Planet. Space Sci., 22, 623-631, 1974.

Roble, R. G., R. E. Dickinson, and E. C. Ridley, Seasonal and Solar Cycle Variations of the Zonal Mean Circulation in the Thermosphere, J. Geophys. Res., 82, 5493-5504, 1977.

Salah, J. E., and J. M. Holt, Midlatitude Thermospheric Winds From Incoherent Scatter Radar and Theory, Radio Sci., 9, 303-313, 1974.

Schunk, R. W., Transport Equations for Aeronomy, Planet. Space Sci., 23, 437-485, 1974.

Schunk, R. W., and A. F. Nagy, Electron Temperatures in the F-Region of the Ionosphere: Theory and Observations, Rev. Geophys., 16, 355-399, 1978.

Smith, P. A., and J. W. King, Long Term Relationships Between Sunspots, Solar Faculae, and the Ionosphere, J. Atmos. Terr. Phys., 43, 1057-1063, 1981.

St. Maurice, J. P., and R. W. Schunk, Diffusion and Heat Flow Equations for the Mid-latitude Topside Ionosphere, Planet. Space Sci., 25, 907-920, 1977.

Stubbe, P., and S. Chandra, The Effects of Electric Fields on the F-Region Behavior as Compared with the Neutral Wind Effects, J. Atmos. Terr. Phys., 32, 1909-1919, 1970.

Young, E. R., D. G. Torr, P. G. Richards, and A. F. Nagy, A Computer Simulation of the Mid-latitude Plasmasphere and Ionosphere, Planet. Space Sci., 28, 881-893, 1980.

APPENDIXES

Appendix A. General Information on Ionosonde Stations

Table 2. Description of Ionosonde Stations.

NAME	GEOGRAPHIC LOCATION (degrees)	MAGNETIC LONGITUDE (degrees)	L-SHELL	LMT (hrs)	LST MERIDIAN (degrees)	SUNRISE LMT/UT (hrs)	SUNSET LMT/UT (hrs)	NO IONOSONDE DATA (yrs)
Akita	39.70 N/140.10 E	206	1.351	UT+9.10	135 E	7.05/21.95	16.95/7.85	None
Canberra	35.30 S/149.00 E	225	1.955	UT+10.34	150 E	5.14/18.80	18.77/8.43	1984 - 87
Hobart	42.90 S/147.30 E	224	2.629	UT+10.34	150 E	4.83/18.49	19.20/8.86	1984 - 87
Khabarovsk	48.50 N/135.10 E	200	1.645	UT+8.74	135 E	7.39/22.65	16.61/7.87	1968, 76, 77, 80, 82 - 83
Ottawa	45.40 N/284.10 E	351	3.347	UT-5.19	75 W	7.20/12.39	16.80/21.99	None
Poitiers	46.57 N/ 0.35 E	81	2.408	UT+0.83	15 E	7.20/ 6.37	16.80/15.97	1966
Sverdlovsk	56.70 N/ 61.10 E	141	2.357	UT+4.77	60 E	7.88/ 3.11	16.00/11.23	1982 - 83
Tomsk	56.50 N/ 84.90 E	159	2.125	UT+6.03	90 E	7.88/ 1.85	16.17/10.14	1972, 76, 79, 81, 83
Townsville	19.63 S/146.85 E	219	1.321	UT+10.00	150 E	5.64/19.64	18.42/8.42	1983 - 87
Yakutsk	62.00 N/129.60 E	194	2.597	UT+8.32	135 E	8.36/ 0.04	15.64/7.32	1965, 80 - 87

Appendix B. Geomagnetic and Solar Data

Table 3. Geomagnetic and Solar Data.

YEAR	F10.7	F10.7A	Ap	R_{12}
1987	69.6	75.4	4.5	10
1986	72.9	73.5	4.3	2
1985	72.6	73.1	6.3	16
1984	100.3	92.4	5.2	58
1983	140.8	170.0	7.3	86
1982	152.2	200.5	4.2	111
1981	161.6	205.1	4.8	114
1980	201.4	212.3	4.4	162
1979	189.2	163.7	7.8	166
1978	94.7	106.4	3.5	49
1977	74.1	73.5	5.2	16
1976	70.9	75.0	5.6	8
1975	75.3	83.0	5.4	19
1974	86.8	77.9	5.5	30
1973	97.6	106.2	5.6	43
1972	101.1	112.9	4.7	65
1971	150.0	152.6	3.5	78
1970	148.9	152.8	4.2	105
1969	158.9	148.3	2.6	110
1968	189.2	163.7	6.7	115
1967	161.6	205.1	3.0	108
1966	94.7	106.4	2.0	27
1965	74.1	73.5	2.6	18

Appendix C. Copyright Permission Request Letters

364 E. 2700 N.
North Logan, Utah 84321
(801) 752-0887 or 750-1955

FEB 24 1989

16 February 1989

Academic Press, Inc.
111 Fifth Avenue
New York City, New York 10003

Dear Sir:

I am in the process of preparing my thesis in the Center for Atmospheric and Space Science Department at Utah State University. I will complete my degree in the Spring quarter of 1989.

I am requesting your permission to include the material which is listed in the endorsement section below. I will include acknowledgements and/or appropriate citations to your work as required by U.S copyright laws. If further requirements are necessary for inclusion of these works in my thesis, please make appropriate annotations in the endorsement section.

Please indicate your approval of this request by signing in the space provided, and attaching any other form or instructions which are necessary to confirm permission. If a reprint fee is required for the use of your material, please indicate that as well. If you have any questions, please call me at the numbers given above. Written correspondence should be sent to the address listed above so as to ensure a prompt response to your requests for use of the listed material.

Please send your response to this request immediately as I am in the final stages of completing my thesis and completion of additional degree requirements. If you are not the copyright holder, please forward my request to the appropriate person or institution.

Thank you for your cooperation.

Ronald L. Breninger

I hereby give permission to Ronald Breninger to reprint the following material in his thesis. A reprint fee of $_____ is/is not required for use of this material.

Banks, P. M., and G. Kockarts, Aeronomy: Part A, Academic Press, 1973.

Figure 1.2 p.3

PLEASE TURN OVER

_____ _____
(Signature) (Date)

Center for Atmospheric and Space Science
Utah State University
Logan, Utah 84322

February 28, 1989

PERMISSION GRANTED, provided that 1) complete credit is given to the source, including the Academic Press copyright line; 2) the material to be used has appeared in our publication without credit or acknowledgement to another source and 3) if commercial publication should result, you must contact Academic Press again.

Martha Stroesberger
Contracts, Rights and Permissions
ACADEMIC PRESS, INC.
Orlando, Florida 32887

364 E. 2700 N.
North Logan, Utah 84321
(801) 752-0887 or 750-1955

Pergamon Press, Inc.
Maxwell House
Fairview Park
Elmsford, New York 10523

16 February 1989

Dear Sir:

I am in the process of preparing my thesis in the Center for Atmospheric and Space Science Department at Utah State University. I will complete my degree in the Spring quarter of 1989.

I am requesting your permission to include the material which is listed in the endorsement section below. I will include acknowledgements and/or appropriate citations to your work as required by U.S copyright laws. If further requirements are necessary for inclusion of these works in my thesis, please make appropriate annotations in the endorsement section.

Please indicate your approval of this request by signing in the space provided and attaching any other form or instructions which are necessary to confirm permission. If a reprint fee is required for the use of your material, please indicate that as well. If you have any questions, please call me at the numbers given above. Written correspondence should be sent to the address listed above so as to ensure a prompt response to your requests for use of the listed material.

Please send your response to this request immediately as I am in the final stages of completing my thesis and completion of additional degree requirements. If you are not the copyright holder, please forward my request to the appropriate person or institution.

Thank you for your cooperation.

Ronald L. Breninger

I hereby give permission to Ronald Breninger to reprint the following material in his thesis. A reprint fee of $_____ is/is not required for use of this material.

Bradley, P. A., and J. R. Dudeney, A Simple Model of the Vertical Distribution of Electron Concentration in the Ionosphere, J. Atmos. Terr. Phys., 35, 1973.
Figure 1 p. 2133

Young, E. R., D. G. Torr, P. G. Richards, and A. F. Nagy, A Computer Simulation of the Mid-Latitude Plasmasphere and Ionosphere, Planet. Space Sci., 28, 1980.
Figure 1 p. 884

_____ _____
(Signature) (Date)

Center for Atmospheric and Space Science
Utah State University
Logan, Utah 84322

PERGAMON PRESS, INC.

February 28, 1989

Ronald L. Breninger
384 E. 2700 North
North Logan, Utah 84321

Dear Mr. Breninger:

With reference to your attached request to reprint/reproduce material from a Pergamon journal, we herewith grant permission to do so, provided:

1. The material to be reproduced has appeared in our publication without credit or acknowledgement to another source.

2. Suitable acknowledgement to the source be given, preferably as follows:

   Reprinted with permission from [Journal Title, Volume Number, Author(s), Title of Article], Copyright [Year], Pergamon Press plc.

3. The author's approval in writing be obtained (the address or affiliation that appears in the journal is the most current available).

4. A copy of your work is submitted upon publication to the Journal Permissions Department.

This permission is for one-time use and for use in editions for the handicapped.

We only grant non-exclusive world English rights. If an individual wants rights for all languages, it would have to be applied for separately.

Sincerely,

Joan M. Yurczak
Journals Permissions

MATERIAL TO BE REPRINTED/REPRODUCED AND TO BE USED IN:

As per your attached letter(s).

Enclosure: original request(s) for permission

Maxwell House, Fairview Park, Elmsford, NY 10523 (914) 592-7700 Fax: (914) 592-3625 Telex: 13-7336 Cables: PERGAPRESS ELMFD
Member of the Maxwell Communication Corporation Group of Companies

Journal of Geophysical Research

The editors of JGR welcome original scientific contributions on the physics and chemistry of the Earth, its environment, and the solar system. Papers on aeronomy and magnetospheric physics, planetary atmospheres and magnetospheres, interplanetary and external solar physics, cosmic rays, and heliospheric physics are published in JGR–Space Physics. Brief reports of 12 or fewer pages of main text and 5 or fewer figures are encouraged and are processed more rapidly. Four copies of the typescript should be submitted to

Thomas J. Birmingham, JGR
Code 695.1
NASA Goddard Space Flight Center
Greenbelt, MD 20771
(301) 474-4042
Editor's Assistant: Sandra Barnes

Papers on the physics and chemistry of the Earth, its environment, and the solar system should be submitted to any one of the following editors for JGR–Solid Earth and Planets: William M. Kaula, Editor-in-Chief, Department of Earth and Space Sciences, University of California, Los Angeles, California 90024; Ross S. Stein (Geodesy and Tectonophysics), U.S. Geological Survey, Menlo Park, California 94025; Kenneth A. Hoffman (Geomagnetism and Paleomagnetism), California Polytechnic State University, San Luis Obispo, California 93407; Steven W. Squyres (Planetology), Cornell University, Ithaca, New York 14853; John A. Orcutt (Seismology and Tectonophysics), Scripps Institution of Oceanography, La Jolla, California 92093; Seth A. Stein (Tectonophysics and Seismology), Northwestern University, Evanston, Illinois 60201; Dean C. Presnall (Volcanology, Geochemistry, and Petrology), University of Texas at Dallas, Richardson, Texas 75083-0688. Papers on the ocean and marine atmospheric boundary layer should be submitted to one of the following editors of JGR-Oceans: James J. O'Brien, Editor-in-Chief, Box 2254, Tallahassee, Florida 32316; Larry P. Atkinson (Physical Oceanography), Old Dominion University, College of Sciences, Department of Oceanography, Norfolk, Virginia 23529-0276; Richard W. Eppley (Biological Oceanography), Institute for Marine Research A-018, Scripps Institution of Oceanography, La Jolla, California 92093; W. J. Jenkins (Chemical Oceanography), Department of Chemistry, Clark 4, Woods Hole Oceanographic Institution, Woods Hole, Massachusetts 02543. Papers on atmospheric science should be submitted to Shaw Liu, JGR-Atmospheres, NOAA/ERL, Aeronomy Laboratory, 325 Broadway, Boulder, Colorado 80303.

Publication Charge Policy. The page charge income received for JGR helps support rapid publication, allows more pages per volume, and makes possible the low subscription rates which result in a circulation of about 5000 issues, about half going to libraries, where wider distribution is afforded. The publication charge for full articles typeset by AGU is $140 per printed page. AGU will typeset only those articles for which the AGU typeset rate is paid. If the author provides final typewritten or typeset copy, prepared according to AGU specifications, the publication charge is $72 per printed page. Authors who cannot obtain funding should contact the AGU for information on the page-charge experiment. Those authors who can honor the regular publication charges receive 100 reprints. Foldouts and color figures may be published if they are necessary to the proper presentation of material. The additional cost for these services must be borne by the author. Check with the AGU reprint department for current prices.

Microform Publication. Authors are encouraged to submit concise papers. To reduce publication expense and still allow for complete reporting of work, AGU provides a microfiche deposit service to its authors. AGU will print typeset summaries of papers and place the manuscript of the full paper on microfiche at the following rates: no charge for the first two typeset pages, $250 for each additional typeset page, and a $19 deposit charge for each 96 pages or fraction thereof placed on microfiche. In addition to original papers for which summaries have been published in the journal, materials well suited to micropublication include lengthy mathematical derivations, tables of data, computer printouts, and appendices. Photographs with a wide tonal range are not suitable for microfiche. Detailed information on preparing copy for microfiche is available from the AGU production office. All supplemental material is incorporated in the microform editions of the journal and therefore is a part of the archived literature. Material published in microfiche can be ordered by individuals at a nominal cost from the AGU business office.

Subscriptions. All AGU members may subscribe to the *Journal of Geophysical Research* in printed or microfiche editions for their personal use. Special subscription rates are available to libraries, reading rooms, multiple-use institutions, and individual nonmembers (for personal use). Interested subscribers should contact AGU for specific subscription information. Call toll free: 800-424-2488, 9–5 weekdays.

Changes of Address and Claims. Send address changes to AGU circulation department; allow 5 weeks advance notice. Claims for missing issues will not be honored because of insufficient notice of address change, loss in mail unless claimed within 90 days for U.S.A. and 150 days for other countries from last day of month of publication, or such reasons as 'missing from files.'

For assistance with accepted manuscripts, submission requirements, or AGU publication policy, contact Michael Connolly, Production Coordinator, at (202) 462-6903.
Judy C. Holoviak, Director of Publications
AGU Office. Address all correspondence to the appropriate department at the American Geophysical Union, 2000 Florida Avenue, N.W., Washington, D.C. 20009. Telephone (202) 462-6903. TWX 710-822-9300.

Journal of Geophysical Research, JGR (USPS 368000) is published weekly for $301 per year (for AGU members' personal use) by the American Geophysical Union, 2000 Florida Avenue, N.W., Washington, D. C. 20009. Second-class postage paid at Washington, D. C., and additional offices. POSTMASTER: Send address changes to *Journal of Geophysical Research*, American Geophysical Union, 2000 Florida Avenue, N.W., Washington, D. C. 20009.

UNITED STATES DEPARTMENT OF COMMERCE
National Oceanic and Atmospheric Administration
Environmental Research Laboratories
325 Broadway
Boulder, Colorado 80303-3328

E/GC2 D20354
September 14, 1988:DGS

Dr Kent Miller
Utah State University
Center for Atmospheric
and Space Sciences
Logan, Utah 84322-44-5

Dear Dr. Miller:

I am enclosing the final part of your data re st (no. E/GC2 D20354) The copies, of foF2, FM3000F2, and foe tab sheets are all that are available. Some stations are not complete and you may assume the station had equipment problems and was not operating at that time.

Please be advised that you and your colleagues are always welcome to use the Boulder Data Center when you are in town.

Thank you for your patience in getting the data together and copied. If you find any of it not readable please call and I will check the original data to see if we can help.

Sincerely yours,

Doris Stansell

Mrs. Doris Stansell
Ionosphere Branch
NOAA/NGDC E/GC2